

Journal of Visualized Experiments

Array tomography workflow for the targeted acquisition of volume information using scanning electron microscopy --Manuscript Draft--

Article Type:	Invited Methods Article - JoVE Produced Video
Manuscript Number:	JoVE61847R3
Full Title:	Array tomography workflow for the targeted acquisition of volume information using scanning electron microscopy
Corresponding Author:	Irina Kolotuev, Ph.D. Universite de Lausanne Faculte de biologie et medecine Lausanne, SWITZERLAND
Corresponding Author's Institution:	Universite de Lausanne Faculte de biologie et medecine
Corresponding Author E-Mail:	irina.kolotueva@unil.ch
Order of Authors:	Irina Kolotuev, Ph.D. Dr. Tilman Franke
Additional Information:	
Question	Response
Please indicate whether this article will be Standard Access or Open Access.	Open Access (US\$4,200)
Please indicate the city, state/province, and country where this article will be filmed . Please do not use abbreviations.	Lausanne, Switzerland
Please confirm that you have read and agree to the terms and conditions of the author license agreement that applies below:	I agree to the Author License Agreement
Please specify the section of the submitted manuscript.	Biology
Please provide any comments to the journal here.	We could not upload the Supplementary movie 1

TITLE:

Array Tomography Workflow for the Targeted Acquisition of Volume Information Using Scanning Electron Microscopy

AUTHORS AND AFFILIATIONS

Tilman Franke,¹ Irina Kolotuev²

¹Thermo Fisher, 82152 Planegg, Germany

²Universite de Lausanne, Bâtiment Biophore, Quartier Sorge, CH-1015 Lausanne, Switzerland

Corresponding Author:

Irina Kolotuev (irina.kolotueva@unil.ch)

Email Address of Co-author:

Tilman Franke (tilman.franke@thermofisher.com)

KEYWORDS:

serial sectioning, array tomography, automatic acquisition/ imaging, volume electron microscopy, correlated microscopy, scanning electron microscopy, large field acquisitions

SUMMARY:

We describe the preparation of ribbons of serial sections and their collection on large transfer support for use as Array Tomography samples, along with automated imaging procedures in a scanning electron microscope. The protocol allows screening, retrieval, and targeted imaging of local, rare events, and the acquisition of large data volumes.

ABSTRACT:

Electron microscopy is applied in biology and medicine for imaging of cellular and structural details at nanometer resolution. Historically, Transmission Electron Microscopy (TEM) provided insight into cell ultrastructure, but in the recent decade, the development of modern Scanning Electron Microscopes (SEM) has changed the way of looking inside the cells. Even though the resolution of TEM is superior when protein-level structural details are needed, SEM-resolution is sufficient for the majority of the organelle-level cell biology-related questions. The advancement in technology enabled automatic volume acquisition solutions such as Serial block-face imaging (SBF-SEM) and Focused ion beam SEM (FIB-SEM). Nevertheless, to this day, these methods remain inefficient when the identification and navigation to areas of interest are crucial. Without the means for precise localization of target areas before imaging, operators need to acquire much more data than they need (in SBF-SEM), or, even worse, prepare many grids and image them all (in TEM). We propose the strategy of "lateral screening" using Array Tomography in SEM, which facilitates the localization of areas of interest, followed by automated imaging of the relevant fraction of the total sample volume. Array tomography samples are conserved during imaging, and they can be arranged into section libraries ready for repeated imaging. Several examples are shown in which lateral screening enables us to analyze structural details that are incredibly challenging to access with any other method.

INTRODUCTION

Despite the importance of EM-related techniques, the effort required to master them keeps the entire field restricted to a small number of specialists. One significant difficulty is the identification and retrieval of a Region of Interest (ROI) in the samples preserved for EM. The appearance of the same sample considerably differs when analyzed by optic microscopy and after processing for EM observation. The changes for chemically prepared samples include the anisotropic sample shrinkage after the dehydration steps (~10% in each dimension) and the loss of fluorescence when using osmium in the fixation and staining protocol (**Figure 1A**). For the ultrathin sectioning, the samples are embedded in epoxy or acrylic resins using different strategies (**Figure 1B**). For successful results of this preparation, the entire sample must be fractionated into pieces that do not exceed 1 mm x 1 mm. To meet standard Transmission Electron Microscopy (TEM) observation conditions' requirements, this tiny portion of the sample is further sectioned to 50-150 nm thick slices. The resulting grayscale images show tissue organization and organelle structure of a minute fraction of the entire sample at greater detail than any other microscopy technique (**Figure 1C**). A typical TEM dataset provides 2D information, theoretically extrapolated to understand the processes naturally occurring in a 3D space in cells and tissues. **Figure 1D** presents the challenge of ultrastructural volumes acquisition: if a cube of side 1,000 μm is sectioned at 50 nm thickness, 20,000 sections will be required to cover the entire volume; for a 500 μm side cube, it will be 10,000 sections. To cover a 50 μm x 50 μm x 50 μm volume, 1,000 sections "only" might be necessary. Obtaining this volume manually is practically impossible and extremely challenging to perform with automation. If, in addition to sample depth, we need to cover the entire surface of such hypothetical cubes, the coverage of 1 μm^2 surface at reasonable resolution becomes a serious logistic issue (**Figure 1E**). While for the extraordinary large-scale projects, such as connectomics approaches, the large number of sections is crucial, for the majority of the "mundane" EM projects, generating more sections required for the observation presents a significant disadvantage.

There are several methods to acquire 3D ultrastructural information: serial sectioning Transmission Electron Microscopy (TEM), TEM tomography, Array Tomography (AT), Serial Block Face Imaging Scanning Electron Microscopy (SBF-SEM), and Focused Ion Beam Scanning Electron Microscopy (FIB-SEM). Principal differences between these methods are the sectioning strategy and whether the image acquisition is coupled to section generation¹. In serial sectioning TEM, sequential sections are collected on slot grids, TEM images are generated from these sequences and aligned²⁻⁵. In TEM tomography, tilt series from 150-300 nm sections on a grid, and when coupled to serial sectioning, provide a very high resolution, though relatively small volumes⁶⁻⁸. The AT approach uses physical sectioning with diverse manual and semi-automatic manners of sections collection on relatively large support, such as glass coverslip, silicon wafers or a special tape. For image acquisition, the support is analyzed in SEM, with diverse image acquisition strategies are available⁹⁻¹⁵. For SBF-SEM, physical sectioning is achieved using a mini-microtome with a diamond knife set directly inside the SEM chamber, with the SEM image generated from the surface of the resin block¹⁶⁻¹⁹. For FIB-SEM, ion source removes thin layers of the sample, followed by automatic imaging of the exposed surface by the SEM^{20,21}. TEM-tomography and the AT generate physical sections, which can be re-imaged if necessary, while FSBF-SEM and FIB-SEM eliminate the section after imaging. A recent

combination of physical sections imaged by a multi-beam SEM provides a combination of methods that solves the "bottleneck" issue of the speed of image acquisition²². Each of these techniques has revolutionized the way EM data can be obtained and analyzed, and each approach has its practical impacts related to a given research question.

Given the nature of the preparation and the scale of the ultrastructural dimensions, it is not straightforward to predict where a specific target structure is located in the sample block (**Figure 1D,E**). One solution for the ROI localization is recording the images from the entire block at the desired resolution from the beginning. The structures of interest can be in the acquired data volume when away from the microscope. Acquisition time and data handling associated with this strategy are problematic. It is desirable to reduce the amount of recorded data, especially if the ROIs are much smaller than the tissue block, i.e., if the objects of interest are specific types of cells (not whole organs). Different correlative light and electron microscopy techniques (CLEM) can be successful when the fluorescence is preserved and localized before or after preparation within the same sample²³⁻²⁹. Nevertheless, many cellular structures are recognizable even without fluorescence correlation, only based on the known ultrastructure. For these cases, we believe that lateral screening Array Tomography provides a balance tradeoff between the effort invested in ROI localization and the ultrastructural information quality. Using this strategy, a sub-set of sections on the wafer are screened within regular intervals, which can be established based on the ROI's size and nature. Once ROIs are found, data acquisition is set up in a continuous series of sections starting before and ending after the anchor section, collecting the relevant information in a targeted manner.

We present protocols for AT that simplify and accelerate the acquisition of regions or events of interest in numerous sections and yield better-aligned image volumes. Lateral screening and multistep acquisition produce data with very high resolution in precisely targeted regions. The procedure we describe addresses several challenges of 3D EM data acquisition, as it provides for: compatibility with a broad range of specimens without fundamentally changing the sample preparation workflow; targeted localization for sectioning and SEM acquisitions; reduced time and effort during setup; imaging of regions in multiple sections with better alignment of the resulting volumes; and a smooth stitching and alignment procedure to compile different images into a stitched mosaic picture. We chose to demonstrate the strength of our method with several samples from published and ongoing projects. We believe that this approach can significantly facilitate the generation and acquisition of targeted EM data, even for investigators with limited EM experience.

PROTOCOL:

NOTE: Sample preparation methods are described elsewhere^{14,30}, and are not covered in this publication. In short, the examples shown were chemically fixed with glutaraldehyde, post-fixed with 1% OsO₄, then treated with 1% aqueous uranyl acetate before embedding in the embed resin. Alternatively, samples can be prepared using high-pressure freezing, freeze substituted with 0.1% uranyl acetate in acetone, and embedded in acrylic resin. Sample blocks were prepared using a flat embedding method that permits a clear view of the sample, facilitating its orientation for the sectioning (**Figure 1B**).

1. Array generation procedure

1.1. Embedded sample orientation and trimming

1.1.1. Using the binocular/microscope, identify and mark the ROI on the embedded block surface by lightly scratching the block's surface with a razor blade. This will help to orient the sample inside the ultramicrotome and will reduce the sectioning surface.

1.1.2. Clamp the sample on the ultramicrotome holder (**Figure 2A**).

1.1.3. Trim the resin around the sample, first with the razor blade (rough trimming) and continue with the diamond trimming tool (fine trimming; **Figure 2A**). Use knives with 20° or 90° edge inclination to ensure that the top and bottom surfaces of the block are parallel to the knife's cutting edge.

NOTE: This step is critical for serial sectioning and acquisition of straight ribbons.

1.1.4. Mix xylene and glue in 3:1 proportion. With an eyelash attached to a toothpick, apply this mixture to the top and the bottom edges of the trimmed block. Let it dry thoroughly.

1.2. Prepare the array mounting support A (i.e., silicon wafers).

1.2.1. Cut the wafer piece using a wafer cleaving tool (EMS), adjusting its size to the project goal. 2 cm x 4 cm is convenient for both light and electron microscopy observations.

1.2.2. Clean the wafer in distilled water to get rid of the debris.

1.2.3. Glow discharge/plasma clean the surface using standard equipment. The precise parameters will depend on the machine used. Start with the parameters for the grids discharge and empirically adjust the time. This step is crucial for a good spread of the sections on the support while sections are drying and should not be omitted.

1.3. Prepare the arrays mounting support B (i.e., glass coverslip)

1.3.1. If planning multiplex immuno-labeling experiments, transfer the samples on a coverslip to better detect the fluorescence signal. To improve coverslip adhesiveness, use a detailed gelatin-coating procedure is described previously⁹.

1.3.2. Increase the conductivity by coating the slides with the indium-tin-oxide (ITO) or gold by evaporation. Keep the prepared coverslips in a clean environment. Glow discharge the samples as described in 0.

2. Sectioning of the sample

2.1. AT knife preparation

NOTE: To generate the arrays, use a modified knife (ATS), designed to facilitate the acquisition of long ribbons. Histo-Jumbo knife can serve for AT sectioning as well.

2.1.1. Attach the needle to the bottom of the knife using the foamy sticky tape and pierce it (**Figure 2B**). Place the knife in the ultramicrotome holder at 0°. Adjust the edge of the knife parallel to the block surface using the standard procedure.

2.1.2. Bring the trimmed block to the edge of the knife in a position ready for sectioning.

2.1.3. Place the wafer/coverslip inside the knife basin and fill it with water to the same level as the knife edge. Let the diamond edge of the knife humidify properly and, if necessary, withdraw water using the attached syringe (**Figure 2C**).

2.2. Array sectioning and transfer

2.2.1. Set the microtome to the desired cutting parameters. With the ATS knife, the range of 50-100 nm and a cutting speed of 0.6-1 mm/s are advisable. Start sectioning (**Figure 2Di**).

2.2.2. Obtain a ribbon of the length that will cover a targeted z-volume and stop the collection. Depending on the block size, homogeneity of the tissue, and type of resin, the ribbon will approximately be straight (**Figure 2D-ii**). Many samples will not produce straight ribbons, despite the invested effort and the type of knife is used.

2.2.3. Depending on the final goal, make one long or several short ribbons aligned side by side. A 2 cm x 4 cm support can conveniently hold 100 to 1,000 sections. The arrangement of the ribbon on the support step is a step that requires dexterity and steady hands. However, the learning curve for this skill is rapidly acquired.

2.2.4. Detach the ribbon from the knife-edge using a clean, non-sticky tip of an eyelash glued on the toothpick (**Figure 2Diii**).

2.2.5. Using the eyelash, gently move the ribbon above the center of the support medium. At this point, use chloroform or heating pen for stretching of the sections if needed. However, remember that this manipulation may induce ribbon breaking and deformation.

2.2.6. Start draining the water by pulling the syringe. For more delicate ribbons or a slower water retraction, let water drip by detaching the syringe from the hose. When the water level is lowering to the wafer level, control the ribbon and reposition it if necessary, by gently pushing the ribbon to the center. After settling the ribbons on the wafer surface, continue draining until the remaining water is completely retracted from the basin.

NOTE: If not using the bottom water retraction ATS knife, carefully reduce the water from the sides of the ATS knife to not induce turbulence.

2.2.7. Leave the sections on the support inside the bath to let dry completely. Depending on the hydrophobicity of the support and environmental humidity level, water will evaporate at a different rate (**Figure 2Div**). It is important to let the sample dry slowly to diminish or altogether avoid all folds on the sample.

2.2.8. Transfer the dry sample to a tightly closed box to protect from dirt contamination and place it to a 60 °C oven for at least 30 min. If required, counterstain sections using heavy metals to enhance the overall contrast.

2.2.9. At the end of the procedure, cautiously clean the knife following the manufacturer's instructions

NOTE: The transfer of multiple or serial sections on a wafer (**Figure 2E**) compared to the transfer on a slot grid (**Figure 2F**) change the EM preparation experience entirely. The uninterrupted sectioning and collection of the sections on single support reduces the amount of sectioning and section collection related mistakes frequent in serial sectioning. The equivalent of 100 sections of 1000 µm x 500 µm collected on one wafer corresponds to 33 slot grids (**Figure 2G**).

3. Sample observation

NOTE: This section describes the workflow steps as implemented using a commercially available software (see **Table of Materials**). Any image acquisition software on any SEM platform can be used, however, the specific user actions will differ and will often be more manual.

3.1. Acquire an overview map of SEM images that reveals section locations on the wafer. A built-in optical camera image helps with defining an SEM image mosaic that covers a ribbon of sections or all sections. Create the mosaic by click-drag with the mouse right on the camera image of the sample and start the **Automatic Acquisition**.

NOTE: Very coarse imaging settings, i.e., 1-2 µm pixel size and 1 µs dwell time suffice. This process is illustrated in **Supplementary Material** (pages 2-7).

3.2. Locate sections with the **Section Finder Auto Detection** function or locate them manually. Section positions and outlines are retrieved automatically with this software based on image matching. For illustration of this process, see **Supplementary Material** (pages 8 - 15).

3.3. In case the overview images do not show ROIs clearly, acquire higher resolution images of sections. Use the **Section Preview** function to create and acquire images automatically. This process is illustrated in **Supplementary Material**, pages 16-18. Imaging settings must be chosen according to the nature and size of the ROI that the user searches for.

3.3.1. To find optimal settings, activate the **Live Imaging** in the microscope control software and navigate to one ROI. Alter imaging settings until the images show ROIs clearly, but image

acquisition is not excessively long. Refer to the microscope manual or training material for guidance.

3.4. Define imaging regions

NOTE: Several different strategies are proposed.

3.4.1. If only a few sections need to be imaged, use the images of sections created so far for navigating to the relevant sections and use the **Zoomable Viewer** that shows all acquired images in their original relative locations to look at all sections. Once a section is found that should be imaged at high resolution, create an imaging region with click-drag. Choose high resolution imaging settings and store the settings in a template. Re-use this template for further sections.

3.4.2. To find particularly small or hard to detect rare events, use the Lateral Screening approach. Manually create an imaging region with high resolution imaging settings on every tenth section or on one section per ribbon and acquire the images. Review the images and mark sections that contain the ROI in the software or take a note.

3.4.2.1. Starting from sections that contain the ROI, navigate forward and backward through the section set and create high resolution imaging regions in the same relative locations for as long as the structure is still visible in the section. This can be done manually or by using the procedure described in the next steps.

3.4.3. Acquire images in more than ten consecutive sections. Click **Start Position Refinement** after zooming the image to increase the precision of registered section locations as described in the manual. Doing so decreases the position variability of image series. The procedure is illustrated and explained in **Supplementary Material** pages 19-21.

3.4.4. Click-drag on any section to define an imaging region while holding down the **Alt** key and select **Create Tile Set Array** from the context menu that opens when the mouse button is released. The software then creates imaging regions in the same relative location in all sections that have been found or marked previously. It is possible to limit imaging to a specific range of sections with the **Section Span** slider.

NOTE: This procedure can be repeated with any number of imaging regions and therefore allows recording many small high-resolution images instead of recording a single larger image on each section.

3.4.5. Once created, set up pixel count, pixel size, tiling layout, pixel dwell time, etc. in each image series as needed. Once imaging series are created and set up, they are all listed in a job cue.

3.5. Configure auto functions and start image acquisition

3.5.1. Create a separate image series for auto functions using the same method as describe in the previous step. Move the image series to a position on the section that contains high-contrast structures.

3.5.2. Set the image series to 1024 x 884 pixels and choose a pixel size corresponding to the highest resolution used in the image series set up in the previous steps. In the list of auto functions, check **Auto Focus** and **Auto Stigmator**.

3.5.3. Select **By Section** in the acquisition sequence controls and make sure the auto functions image is the first item in the list. Start the image acquisition by clicking the **Run** button next to the job cue. These procedures are illustrated in **Supplementary Material**, pages 22-23.

NOTE: It is not necessary to manually pre-focus on each section. During the recording session, whenever the microscope advances to a new section, the auto functions will be executed before all other images are recorded in this section.

4. Data alignment and analysis

4.1. Data export

4.1.1. Ensure that data is saved in .tif format, so there is no need for a dedicated export function. Sort data into a folder structure that corresponds directly to the layers and elements in the Layer Tree.

4.1.2. Once image mosaics have been recorded, use the **StitchAll** function to automatically stitch all tiles.

4.2. Stack alignment and cropping in Fiji

NOTE. Many software packages (free and commercial) can be used to work with Array Tomography data. The steps below are shown with open-source program Fiji³¹ because it is widely available and contains all the required functions.

4.2.1. Import a stack of images (or stitched images) into Fiji as a virtual stack.

4.2.2. If contrast/brightness needs to be normalized, choose **Enhanced Contrast...** from the **Process** menu. Set **Saturated Pixels** to 0.1 or less, and check **Process all Slices**.

4.2.3. From the Plugins menu, choose **Registration | Linear Stack Alignment with SIFT**.

4.2.4. Choose **Rigid** or **Affine** from the **Expected Transformation** drop-down menu. Otherwise, keep the default settings. Start the alignment by clicking **OK**.

NOTE: Loading the data as Virtual Stack allows Fiji to handle stacks of any size. The output of the alignment is created in RAM; however, this can limit the maximum size of stacks that can be

processed. In that case, use **Register Virtual Stack Slices**, which is a folder-to-folder implementation of the same registration algorithm. Once registration is complete, load the output data as a virtual stack.

4.2.5. Crop the image stack by clicking **Crop** so that it contains only the ROI.

4.2.6. Save the stack as a single .tif image or series of .tif images.

NOTE: Critical steps of Array Tomography are shown in **Figure 3**.

REPRESENTATIVE RESULTS

The examples below aim to demonstrate the versatility of the recommended workflows. The case study illustrations are projects for which we had difficulty obtaining satisfying results with any other techniques. We chose *Drosophila* adult to illustrate typical challenges one might encounter with numerous types samples. This tubular organ of about 6mm long, 500-1000 μm in cross-section, is divided into different regions with a unique function and cellular composition (**Figure 4A**)³². Depending on the sectioning orientation, the dimensions of the gut profile and its appearance on the section vary. Either transversely or longitudinal orientated sections are relatively large, and only a couple can be placed on a single TEM grid (**Figure 2F**). Only a small portion of the tissue can be imaged in the FIB, and for the SBF-SEM, the difficulty is similar to any non-homogeneous samples. AT provides an efficient tradeoff for the analysis of such samples and flat embedding facilitates the ROI localization. Careful trimming the excess of resin around the selected area (**Figure 4B**) is important for efficient collection of the arrays from the relevant area (**Figure 4C**). Hundreds of sections can be collected on a single wafer sequentially or randomly (**Figure 4D**). Depending on the research question, sample screening and acquisition will require a different strategy, which we arbitrary divided into several scenarios. To illustrate different presented scenarios in a more targeted way, we chose several case studies from the different research project.

Analysis of numerous randomly distributed large structures 1-10 μm range (**Figure 4E**)

Frequently, ultrastructural data are required to validate a hypothesis that arose from several experimental approaches, comparing a standard and experimentally altered condition. In these cases, several sections are typically randomly collected on grids and screened to localize and image the areas of interest. This tactic is usually less systematic and limited to a small number of analyzed sections. We suggest recording overviews of tens/ hundreds of medium-resolution sections from a given ribbon (**Figure 4D**). For typical sections of 70 nm, 200 sections will span approximately 14 μm , which will contain numerous cells, either entirely or partially, completed within half an hour. As the first step, the low-resolution overview of the entire ribbon is recorded, and the overview helps to omit the sections that show preparation artefacts (e.g., folds, dirt). After, the acquisition can be performed manually or automatically directly on selected parts of the section, or an entire section, using single or mosaic imaging, followed by stitching (**Figure 4E**). After, images from the selected area can be acquired using high-resolution parameters. For example, mitochondria, nuclei, and microvilli can benefit from such a statistically improved method (**Figure 4Ei-iii**).

Analysis of multiple small, sparsely distributed structures 500-1,000 nm range (Supplementary Movie 1)

In this scenario, the ROI cannot be simply identified in a low-magnification overview scan, and high-resolution images are needed. In conventional TEM samples, the tedious zooming in and out of the section is necessary until the required feature is found. Often, imaging several independent locations in multiple samples is more relevant statistically than the generation of a single large volume. In such cases, the complexity of manual acquisition grows exponentially. Though several TEM solutions enable the automatic acquisitions or the screening of multiple grids, the size of the grid and serial sectioning challenges frequently make the approach incompatible for many samples. For similar cases, we generate a complete medium-resolution map of an overall ROI in multiple sections at a resolution sufficient to identify the structures of interest. During this lateral screening step, it is advisable to leap several sections at a time, aiming to hit at least a part of the structure of interest when approached randomly. This will largely depend on the overall dimensions of the structure: e.g., if the overall size of the structure is 500 nm and sections are 50 nm thick, at least nine sequential sections in a row will likely contain a portion of the structure of interest. This way, the skipping of 6-7 sections shall be efficient for finding many different kinds of structures in multiple areas. Automatic acquisition of the resolved mosaic maps of selected sections enables careful screening of these sections after their acquisition. Once such a high-resolution map is acquired, several ROIs can be cropped out or used to define additional local imaging areas on ROIs (**Supplementary Movie 1**). Golgi, centrioles, junctions, microtubules, different types of vesicles are good examples of the structures that might benefit from this scenario (**Supplementary Movie 1**).

Analysis of sparsely distributed large ROIs in large samples (Figures 4F-4H)

This scenario involves rare events, which are frequently described as "a needle in a haystack" in which the problem is not in ROI identification but its localization. For many samples correlative approach is not a valid option, yet frequently the ROI has a revealing ultrastructure and, when localized, can be identified with high reliability. For these samples, it is essential to apply multilevel acquisition, starting with the pre-screened samples with tens to hundreds of sections at medium resolution. In the software used here, there are two different strategies for obtaining image sets of multiple sections: Recording the Preview images at a higher resolution or acquiring an Array Tile Set with suitable settings (**Figure 4F**). Different specialized cell types in the *Drosophila* gut are randomly distributed (e.g. stem, enteroendocrine cells), and thin sectioned at random orientation. Yet they can be visually distinguished after screening the images obtained using high-resolution parameters either from single sections or as a collection of serial images (**Figure 4G**). After the alignment, the stacks can be rendered using different software solutions (**Figure 4H, Supplementary Movie 2**).

Scenario 1: Intestinal organoids (Figure 5A)

Organoids are fast-becoming one of the most cutting-edge tools of modern life sciences. This near-physiological 3D stem-cell-derived organ model makes possible an accurate study of a range of in vivo biological processes, including tissue renewal, response to drugs, and regenerative medicine. Recently introduced mini-gut tubes³³ open up a new generation of organoid technology, closely resembling in vivo tissue physiology, cell-type composition, and homeostasis, enabling broad perspectives for disease modelling, host-microbe interaction, and

drug discovery. However, when ultrastructural characterization is required, the localization of different cell types in such large tissue using random samples can be challenging. Also, in variable "infection" assays, it is crucial to ensure that the analysis reveals different developmental stages that affect the tissue. For such studies, statistically significant coverage of the sample is central, yet hard to achieve using the traditional TEM on-grid approach. AT-scenario 1 is beneficial in such cases: many sequential sections can be generated on a wafer (**Figure 5Aii**) and screened using low-resolution parameters to localize the general areas of interest (**Figure 5Aiii**; arrows). These areas can be targeted for further analysis using advanced acquisition parameters (**Figures 5Aiv** and **Figure 5Av**). When a relevant structure is detected (typically a cluster of 5-10 sections once in every 100-300 sections), it is easy to concentrate on each of the structures of interest and acquire single images manually or use the automation features to acquire image volumes across multiple sections.

Scenario 2: *Drosophila* pupal notum (Figure 5B)

Studying cell division and the mechanisms that control progression through the cell cycle is crucial to understanding both standard and altered processes in multicellular organisms. Information that exists is frequently derived from unicellular systems; however, this solution lacks the critical context of the 3D interactions between the cells in a tissue. A single-cell monolayer of the notum, the developing back of the *Drosophila* larva, is a perfect model for the interaction between the epithelial cells in general and cell division in particular³⁴. It is an established model for molecular and cellular interactions studies using the combination of the data available by fluorescent microscopy and genetic manipulations. Abscission, the last step of cell division, assures the final separation between two dividing cells, and characterizing the structural changes that occur during abscission is essential to our understanding of mitosis. However, mitotic divisions in the notum are not easy to localize on the ultrastructural level: the cells are relatively large, compared to the abscission zone (**Figure 5B**). The ratio between the overall size of the abscission zone and the surface of the section to cover is large (**Figure 5Bi**). Even though it possible to localize the abscission zone using the TEM or SBF-SEM methods³⁵, the task is laborious. With this scenario, the automatic medium-resolution overview images of the leaps of 20-40 sections can be used to localize the dividing cells (**Figure 5Bii**). When such cells are identified, the sections serve as the anchor for closer examination of the sections in the vicinity, and numerous dividing cells can be found and selected for further analysis. This way, the abscission zone can be located and imaged in its entirety (**Figure 5Biii**). Depending on the question, single high-resolution images or 3-7 image sequences can be collected to cover the depth of the structure (**Figure 5Biv**).

Scenario 3: Mouse tanycyte neurons (Figure 5C)

The mouse provides a well-established model for brain development and is well documented on different levels, including by EM. Even though different automated serial-block-face methods have been used extensively to study brain tissue, there are cases where AT is better adapted to collect the necessary data. The hypothalamus is a well-established neuroscience model, a part of the brain that contain multiple neuronal types functions. Hypothalamic tanycytes represent a particular subset of ependymogial cells lining the bottom of the third ventricle, with unusually long processes (up to 300 μm) and large endfeet ($\sim 5 \mu\text{m}$)³⁶. This makes them inconvenient for the analysis by either TEM or FIB methods. The task is further complicated when several

independent tanycytes need to be localized and analyzed. One of the approaches to facilitate this task can be semi-correlative targeting, in which the fluorescence map is obtained from the fluorescently labeled samples before fixing and embedding for EM. The sectioning is performed on the area captured by combining the positional information from the fluorescence sample and the flat embedded plastic replica. After that, the AT scenario 3 can be used: the high-level overview mosaic images are generated to reveal the regions with tanycyte endfeet clusters. Subsequently, automation features in the software are used to set up the acquisition of sequences of the images from one or several areas in a single image or tiled mode. These images can be analyzed separately, as aligned stacks or rendered after that.

The power of the AT method permits the relatively effortless "upgrade" of data from 2D to 3D: the maps are available from the primary acquisition, and the volumes can be obtained from the selected area and its vicinity. The resulting stack can be aligned and subsequently rendered. It is essential to determine beforehand which resolution and image quality are needed to find ROIs. Imaging should enable recognizing the ROIs, but not beyond this value because acquisition time scales proportionally to pixel dwell time and the inverse square of pixel size.

FIGURE AND TABLE LEGENDS

Figure 1: Challenges of EM sample preparation and volume acquisition. (A) The loss of fluorescence and shrinkage happens due to a high heavy metal concentration and dehydration during sample preparation. (i) A schematic drawing of a specimen observed under LM (ii) the same specimen prepared for EM, which becomes completely opaque and loses around 10% of its volume. (B) Sample embedding is typically done using epoxy or acrylic resins. Traditional blocks (i) can be successfully used for homogeneous samples that do not require a particular orientation. Flat blocks (ii) are helpful when it is essential to target and orient under the microscope, a precise area aimed for sectioning, e.g., in non-homogeneous samples or correlative microscopy procedures. (C) Of the entire sample volume, only a limited fraction is represented on a single 50 nm section, providing a 2D image of a 3D sample, frequently in an unfamiliar orientation. (D) To illustrate the problem of recording overly large volumes versus precise targeting, we chose three concentric cubes with the faces of 1000, 500, and 50 μm are organized to include a hypothetical 1000 x 500 x 500 μm sample (dark maroon). If such hypothetical sample cubes are thoroughly sectioned with 50 nm slices, to cover the entire volume, it will require a total of 20,000, 10,000, and 1,000 slices, and 800 tb, 100 tb, and 100 gb, accordingly (imaging resolution 5 nm x 5 nm x 50 nm, 8 bit data). This shows the importance of planning the acquisition of EM data only to acquire the minimum necessary volume. (E) To cover a large sample surface area in high resolution presents a problem similar to that of large volume. Tiling several high-resolution images into one is a helpful solution for such a problem. However, to cover a 1 mm x 1 mm surface using the 2024 x 1048 frame in 10,000x magnification will require a vast number of tiles, which can become challenging to stitch. Further, if sections are variably compressed or distorted during cutting, the resulting data stacks become almost impossible to align.

Figure 2: The workflow for the direct generation of the arrays of sections on large support. (A) For tight trimming using the trim tool, blocks are secured inside the microtome holder. This step

helps to ensure parallel sides of a block and also reduces empty resin around the sample. **(B)** A modified knife for AT sections acquisitions. A large boat facilitates the transfer of the sections and their manipulation during sample sectioning and transfer on the support. A large basin enables the manipulation of the sections; the draining system limits the movement of the ribbons during the draining step, the flat bottom makes gradual drying of the support reliable. **(C)** The knife, ready for sectioning with a glow-discharged wafer placed at the bottom of the basin and water leveled to the edges. The construction of the knife keeps the needle embedded, without interfering with the support. **(D)** Array generation, top view on the microtome sectioning area. (i) The first sections are usually easy to obtain as they stick to one another and form a regular ribbon. (ii) When more sections are added to the ribbon, and it becomes longer, the ribbon loses its stability and frequently curves. It is crucial to keep the sequence tracks organized in sequence in preparation for the image acquisition step. (iii) When a ribbon of sections reaches the desired length, it is carefully detached from the knife-edge using an eyelash. (iv) Water is drained from the basin; the wafer remains inside until it is entirely air-dry. This step is essential, as it helps to straighten the sections and avoid the formation of the micro folds. The wafer is placed in the oven at 60°C for at least 30 min to attach the sections on support. **(E)** Example wafers with the transferred sections. Though it is convenient to obtain straight and accurate ribbons, actual samples prevent the formation of such ideal ribbons in most cases. Nevertheless, even "sloppy" ribbons are very informative for the vast number of cases, and the importance of the "neat" ribbon will depend on a research strategy for which the sections are collected. Scale bar 1 cm. **(F)** Example slot grids with the serial sections. Even when many sections are collected on one grid, it is still a tiny fraction of what can be collected on a single wafer. The skill required to master the transfer of the sections on a grid (slot grid in particular) represented a significant bottleneck for mastering electron microscopy sample preparation. Scale bar 500 μm . **(G)** No matter which section collection method was used, the strengths of the AT approach is the relative ease of generation of sequential sections, compared to the on-grid collection. If a 1000 μm x 500 μm sample block is considered, there is no problem to fit around 100 sections on a 2 cm x 4 cm wafer (i). The same size sections on a slot grid will fit only three sections/grid at maximum (ii). We provide a scaled image to show how many grids might be required to cover the same number of sections, not mentioning the difficulty of collecting serial sections on the grid. Scale bar = 1 cm.

Figure 3: Critical steps of Array Tomography workflow. Schematic of the workflow for the unattended acquisition of high-resolution image stacks. All preparatory steps are automated (green gear symbols) and do not require any actions to be performed manually, section by section. Image stacks can be aligned in any image analysis software capable of automatic rigid or affine alignment.

Figure 4: Three acquisition scenarios with *Drosophila* adult gut as a demonstration model. **(A)** drawing of a dissected *Drosophila* midgut, with three major regions designated by different colors: anterior, middle, and posterior. **(B)** Trimmed flat block in which a gut is oriented for transverse sectioning. Note that the empty resin amount is carefully balanced around the tissue containing the region of interest (white rectangle). **(C)** Transverse serial sections are floating on the water surface inside the basin of the AT knife. All images were acquired in Secondary electron SEM mode using the mirror detector with the inverse contrast. **(D)** Stitched mosaic

image of transverse serial sections on a wafer. Scale bar is 1000 μm . (E) Cross-section through *Drosophila* gut. Scale bar 20 μm . The image is a stitched mosaic of 7 x 7 mid-range images. Insets – higher magnification and resolution images of the specific regions of interest: (ii) nucleus, (iii) brush border, and (i) mitochondria. Scale bar 5 μm for all. (F) A mid-range image of a transverse section through the gut that is targeting the location of developing cells (square). Scale bar is 20 μm . (G) The targeted array of serial sections collected based on the area localized during the analysis of the section present in panel F. Scale bar is 10 μm . (H) The 3D model is rendered based on the 50 sections stack sequence obtained from the targeted serial acquisition in panel G.

Figure 5: Case studies for the AT application scenarios. (A) Localization of different cell structures in the intestinal organoid. (i) Embedded silicon microchip. Scale bar = 200 μm . (ii) A stitched mosaic image of 127 cross-sections through the central part of the chip. Scale bar = 1500 μm (iii) Four low-resolution images of a complete transverse section through the portion of the intestinal organoid. Arrows point to the potential site of interest. Scale bar is 20 μm . (iv) Different ROIs, targeted on low-resolution micrographs selected for further analysis. Scale bar = 10 μm . (v) High-resolution image of the infected cell of interest. Analysis of the same region in the adjacent sections can provide targeted 3D information if required. Scale bar = 5 μm . (B) Midbody localization in *Drosophila melanogaster* pupal notum. (i) A schematic view of a dissected *Drosophila* pupa. Notum exposed for the dissection (beige) after removing the part of the protective cuticle (brown). The black line designates the direction of sectioning (ii) A cross-section through the area presented in the diagram. The image combines 3x7 sequentially taken high-resolution SEM images stitched to one mosaic panel. The black rectangle delimits the area that contains a dividing cell. Scale bar is 15 μm . (iii) A zoomed image on the dividing cell from panel ii. At this magnification and resolution, the midbody is evident (white arrows). The entire section is analyzed to find the dividing cells. Leaping between different ribbons of sections in 20-30 sections intervals during the lateral screening step permits to localize numerous dividing cell pairs. Scale bar is 5 μm (iv) when a dividing cell is localized, sequential images of the midbody collected from four sections around the midbody delimited by yellow square in the panel (iii). Scale bar is 1 μm . (C) Tanycytes endfeet localization in mouse hypothalamus. (i) Fluorescence image of a vibratome slice. Tanycytes express tdTomato fluorescent protein (red). A white rectangle delimits the area of interest. Scale bar 500 μm . (ii) Same vibratome section prepared for EM will be carefully trimmed around the area of interest-based on the indirect correlation of fluorescent information from panel (i). The dotted white line represents the area of ultrathin sectioning. Scale bar is 50 μm for both panels. (iii) Cross-section through the vibratome slice in the area of interest. SEM mosaic image is composed of 75 stitched images. Several sections are targeted by lateral screening and imaged with similar parameters. The sections are analyzed "offline" in order to find the ROI – the tanycyte endfeet. The black rectangle represents the area that contains the tanycyte endfeet. This section will serve as an anchor for further analysis. Scale bar is 15 μm . (iv) High-resolution, high magnification image of tanycyte endfeet surrounding a blood vessel. After the initial localization of the ROI on one section, the z-sequence is collected from the adjacent sections upstream to the anchor section (panel iii). Scale bar 5 μm .

Figure 6: Problems during ultra-microtomy, section collection, and section storage can lead to artefacts. (A) Brain sample sections on a wafer. Most of the empty resin detached from the tissue and folded on itself (sepia). Dashed black box designates an area that is used to contain the entire section. Scale bar 500 μm . (B) A small, local fold on the surface of a 50-nm thick zebrafish section. Scale bar 1 μm . (C) Knife mark on the surface of a 70nm mouse brain section. Scale bar 5 μm . (D) The hair (asterisk) on the surface of the wafer that partially covers a zebrafish muscle section. In yellow, the tissue is targeted for the analysis. In pink, a cell used to serve as a reference for the size of the affected area. Scale bar 50 μm . (E) Zebrafish notochord with wrinkles at the bottom right (black arrows), where dense neural tissue (shadowed in blue) borders on softer muscle tissue and empty resin (black arrows). Scale bar 10 μm . (F) Volume segmentation of a stack of 50 images as in E, showing that this region showed wrinkles in most sections. Dashed polygon outlines the area shown in the G. Scale bar 10 μm . (G) XY view of the same volume segmentation as in F, showing the wrinkles as short black strokes in the right half of the block. Note that the alignment of the stack in the remaining parts of the tissue is not affected by the wrinkles. Scale bar 5 μm . (H) XZ projection of the same area as in G, showing the wrinkles in all 50 sections. Scale bar 5 μm .

Supplementary movie 1: A high-resolution montage image of a cross-section through *Drosophila* anterior midgut. Mosaic image of an inverted SE-MD SEM image. 352 separate image tiles were automatically acquired at 5 nm resolution and stitched to present the entire cross-section. It is possible to zoom in for more details and get an exhaustive coverage of the data, using the same image. Tight junctions, microtubuli, different types of vesicles can be when zooming in. Scale bar is 10 μm .

Supplementary movie 2: *Drosophila* gut cells rendering. Fifty aligned mosaic images of the sections in the area of dividing intestinal cells. IMOD rendering of the cell borders (blue, turquoise, and orange) and nuclei (white).

DISCUSSION:

Electron microscopy gives insight into the ultrastructure of the cells and organisms, for which it is often desirable to image structures of interest in their 3-dimensional context. Despite numerous EM tactics for ultrastructural analysis, there is still no "gold standard" solution. The main reason is the wide variety of samples, many biological questions, which frequently require a tailored approach. The proposed AT workflow is designed to minimize the time necessary for sample processing, data acquisition, evaluation, and storage. Furthermore, the modified knife provides a helpful tool to simplify array acquisition. The compact layout of sections on wafers is convenient, both for the observation and the subsequent storage of the samples. This arrangement enables "Lateral Screening" of samples by horizontally moving from ribbon to ribbon and scanning only one section on each, significantly reducing the time required to localize an ROI. Proposed data acquisition scenarios facilitate the targeting of small and randomly distributed areas. Once found, AT/SEM restricts high-resolution imaging precisely to the volume of interest, whether performed manually or with the help of automatic function. AT for limited volumes can be completed manually, with the operator navigating through the sample and defining imaging regions one by one. The automated module of the software provides a flexible image acquisition strategy for imaging of small areas on large sections. The

automation in this software allows recording large high-resolution images on hundreds of sections, achieving similar volumes as SBF-TEM. Recording overview images of all sections simplifies the ROI localization and reduces the time spent at the microscope. Since the sections are not harmed during the recording of overviews and higher resolution Previews, AT/SEM permits reusing the sample to collect further data of other ROIs or at a higher resolution.

Image acquisition time is one of the most important (and most expensive) aspects of 3D EM and should therefore be considered in the experiment design. While it is unsurprising that imaging large areas takes longer than imaging small areas, it is easy to under-estimate the impact: Depending on the imaging parameters selected, the acquisition time on each section can vary from seconds to hours. Critical imaging parameters include the size of the field of view, resolution, and dwell time. Assuming a target resolution of 10nm per pixel and 1 μ s dwell time, imaging a field of 20 μ m x 20 μ m, 100 μ m x 100 μ m, or 500 μ m x 500 μ m takes 4 seconds, 100 seconds, or 2,500 s to record. We can multiply these per-section imaging times by the number of sections to estimate the time required for the complete imaging job. Long per-section imaging times can be acceptable if the number of sections is small or if microscope tool time is of no concern.

However, it is necessary to limit the recording time to an overnight job or a weekend job in most cases. An equally critical aspect of 3D EM that should be considered, is the amount and structure of the resulting image data. Recording the abovementioned imaging fields in 100 sections generates 400 mb, 10 gb, or 250 gb of image data, respectively; the 500 μ m x 500 μ m images pose the additional issue of being larger than 2 gb each. Many of the software programs used for data evaluation cannot open images of this size.

To reduce imaging time, it is important to choose pixel dwell time to meet the signal-to-noise ratio requirements for the subsequent data evaluation (e.g., reconstruction, tracing), and limit the recordings to defined ROIs. The AT extension of the software facilitates image acquisition in small areas in serial sections. The software supports manual and automatic workflows and many semi-automatic variants: imaging areas can be manually positioned and focused on each section, or the user can use the automatic section finder and position alignment features. Depending on the level of automation chosen and supported by the sample type or imaging goals, the time required for setting up image acquisition in hundreds of sections can take an entire workday (done manually) or only a few minutes. In principle, Array Tomography makes it more challenging than other 3D EM methods to acquire small ROIs; imprecise region placement on consecutive sections must be compensated by acquiring larger areas. For example, if the ROI is 20 μ m x 20 μ m in size and the section-to-section position variability of imaging fields is 10 μ m, one needs to acquire 40 μ m x 40 μ m images in order to be sure that the ROI is fully captured in each image, on every section. Real-world image position variability ranges from 100 μ m to <10 μ m depending on the availability or quality of software features for position alignment or user's patience. With this software, 10 μ m can be achieved without too much manual intervention in most samples.

Like any technique, the AT has several weak points that can influence successful data acquisition, and many are similar to other sectioning-based methods. Lack of homogenous

distribution of empty resin versus tissue can result in curved or broken arrays. In extreme cases, sections can detach from the support (**Figure 6A**). Variable compression or stretching during the cutting process can create folds that can disrupt the sample in variable regions on subsequent sections (**Figure 6B**). Knife marks can appear on the surface of the collected sections using a damaged knife (**Figure 6C**). Differences in sectioning conditions can induce occasional section compression and thickness differences. Dust or dirt particles can land on a section and partially obscure the zone of interest (**Figure 6D**). Image acquisition can fail due to imperfect auto-contrast, auto-focus, and auto-stigmator functions. The positioning of automatically created imaging areas can be variable and may fail to capture the ROI in all sections.

Several problems can arise at the stage of stitching and alignment. The automatic stitching of mosaic tiles acquisitions can fail, for example, because of the large empty space inside the sample. Due to a drastic change in shape in 3D, image stacks can be challenging to register. Specially developed programs (e.g., IMOD, Fiji, TrackEM2, MIB, or MAPS-AT) can facilitate semi-automatic alignment^{31,37-39}. More challenging sections can be manually aligned using photo editing software. Unfortunately, some datasets may be impossible to align correctly.

Large samples are challenging for TEM serial sections fitting onto grids; on the other hand, many projects do not justify long automatic acquisition using FIB/SEM or SBF-SEM. The AT is a straightforward alternative to a tedious serial section TEM where collection and manipulation of serial sections on a wafer are more straightforward than with the slot grids. Several strategies were developed to facilitate the collection of the arrays, and we share our method to expand the existing toolkit. In cases where the identification of the ROI is challenging, AT-SEM provides a fundamental advantage, with the efficient screening of the samples where organelle-scale resolution across 50 to 500 sections is required. For larger volumes, the automatic collection AT strategies can be efficiently collected if more sections are required. AT samples can be re-imaged multiple times, facilitating targeted imaging of high-resolution areas based on previously-acquired overview images. We believe that the targeted analysis and reduced oversampling by AT/SEM proposed here decreases the labor and data storage requirements. Ultimately, libraries of sections can be collected and maintained for later reuse and consultation. For volume acquisition, FIB or SBF-SEM approaches offer an excellent solution whenever the ROI is easy to identify on the block face or if large 3D volumes are needed for the analysis. However, FIB/SBF-SEM are less efficient when the high-resolution stack image has to be collected from a defined ROI in a targeted manner. To conclude, the proposed methods for screening of AT samples and the use of medium resolution overview images allow limiting image acquisition to the relevant parts of the section array. Precise aiming of imaging regions speeds up time-to-data and simplifies data evaluation.

In summary, although the concept of AT/SEM is not novel, its use is still not as widespread as its merits would suggest. Overall, it provides a complementary procedure to other existing EM methods. AT/SEM is compatible with the broadest range of sample preparation protocols and imaging workflows and can be done on any FIB/SEM or SBF-SEM microscope as an accompanying technique. In this paper, we have concentrated on AT for recording ultrastructural data from samples that are less likely to be successfully addressed by other methods. We hope that the described procedure for convenient collection of sections and

considerably automated acquisition strategies will aid in the first attempts for those who have never encountered the method and will help to perfect it for those who already have some experience.

ACKNOWLEDGMENTS:

We want to thank the members of the EM facility of the University of Lausanne for their support during this development of different steps of the AT procedure. We would like to thank Gareth Griffiths, Marta Rodrigues, Urska Repnik, Christel Genoud, Helmut Gnaegi, Einat Zelinger, Paola Moreno-Roman, Lucy O'Brien and Lindsay Lewellyn for discussions during the preparation of the manuscript and critical reading. We want to acknowledge the groups that contributed the samples used to demonstrate the different scenarios: Matthias Lutolf, Michail Nikolaev, Devanjali Dutta, Till Matzat, and Fanny Langlet.

DISCLOSURES:

The author Tilman Franke is an employee of Thermo Fisher that manufactures electron microscopes and piloting programs that are used in the article.

REFERENCES

1. Luckner, M., Wanner, G. From light microscopy to analytical scanning electron microscopy (SEM) and focused ion beam (FIB)/SEM in biology: Fixed coordinates, flat embedding, absolute references. *Microscopy and Microanalysis*. **24** (5), 526-544 (2018).
2. White, J. G., Southgate, E., Thomson, J. N., Brenner, S. The structure of the nervous system of the nematode *Caenorhabditis elegans*. *Philosophical Transaction of Royal Society of London B Biological Sciences*. **314** (1165), 1-340 (1986).
3. Zheng, Z. et al. A complete electron microscopy volume of the brain of adult *Drosophila melanogaster*. *Cell*. **174** (3), 730-743 (2018).
4. Mulcahy, B. et al. A pipeline for volume electron microscopy of the *caenorhabditis elegans* nervous system. *Frontiers in Neural Circuits*. **12**, 94 (2018).
5. Schorb, M., Haberbosch, I., Hagen, W. J. H., Schwab, Y., Mastronarde, D. N. Software tools for automated transmission electron microscopy. *Nature Methods*. **16** (6), 471-477 (2019).
6. Baumeister, W., Grimm, R., Walz, J. Electron tomography of molecules and cells. *Trends in Cell Biology*. **9** (2), 81-85 (1999).
7. Hoog, J. L. et al. Organization of interphase microtubules in fission yeast analyzed by electron tomography. *Developmental Cell*. **12** (3), 349-361 (2007).
8. Weber, M. S., Wojtynek, M., Medalia, O. Cellular and structural studies of eukaryotic cells by cryo-electron tomography. *Cells*. **8** (1) 57 (2019).
9. Micheva, K. D., Smith, S. J. Array tomography: a new tool for imaging the molecular architecture and ultrastructure of neural circuits. *Neuron*. **55** (1), 25-36 (2007).
10. Horstmann, H., Korber, C., Satzler, K., Aydin, D., Kuner, T. Serial section scanning electron microscopy (S3EM) on silicon wafers for ultra-structural volume imaging of cells and tissues. *PLoS One*. **7** (4), e35172 (2012).
11. Hayworth, K. J. et al. Imaging ATUM ultrathin section libraries with WaferMapper: a multi-scale approach to EM reconstruction of neural circuits. *Frontiers in Neural Circuits*. **8**, 68 (2014).

12. Kubota, Y. et al. A carbon nanotube tape for serial-section electron microscopy of brain ultrastructure. *Nature Communication*. **9** (1), 437 (2018).
13. Wacker, I. U. et al. Multimodal hierarchical imaging of serial sections for finding specific cellular targets within large volumes. *Journal of Visualized Experiments*. (133), e57059 (2018).
14. Burel, A. et al. A targeted 3D EM and correlative microscopy method using SEM array tomography. *Development*. **145** (12), (2018).
15. Templier, T. MagC, magnetic collection of ultrathin sections for volumetric correlative light and electron microscopy. *Elife*. **8**, e45696 (2019).
16. Denk, W., Horstmann, H. Serial block-face scanning electron microscopy to reconstruct three-dimensional tissue nanostructure. *PLoS Biology*. **2** (11), e329 (2004).
17. Knott, G., Marchman, H., Wall, D., Lich, B. Serial section scanning electron microscopy of adult brain tissue using focused ion beam milling. *Journal of Neuroscience*. **28** (12), 2959-2964 (2008).
18. Wanner, A. A., Genoud, C., Masudi, T., Siksou, L., Friedrich, R. W. Dense EM-based reconstruction of the interglomerular projectome in the zebrafish olfactory bulb. *Nature Neuroscience*. **19** (6), 816-825 (2016).
19. Smith, D., Starborg, T. Serial block face scanning electron microscopy in cell biology: Applications and technology. *Tissue Cell*. **57**, 111-122 (2019).
20. Kizilyaprak, C., Bittermann, A. G., Daraspe, J., Humbel, B. M. FIB-SEM tomography in biology. *Methods in Molecular Biology*. **1117**, 541-558 (2014).
21. Xu, C. S. et al. Enhanced FIB-SEM systems for large-volume 3D imaging. *Elife*. **6**, e25916 (2017).
22. Hayworth, K. J. et al. Gas cluster ion beam SEM for imaging of large tissue samples with 10 nm isotropic resolution. *Nature Methods*. **17** (1), 68-71 (2020).
23. Maco, B. et al. Correlative in vivo 2 photon and focused ion beam scanning electron microscopy of cortical neurons. *PLoS One*. **8** (2), e57405 (2013).
24. Russell, M. R. et al. 3D correlative light and electron microscopy of cultured cells using serial blockface scanning electron microscopy. *Journal of Cell Science*. **130** (1), 278-291 (2017).
25. Lucas, M. S., Gunthert, M., Gasser, P., Lucas, F., Wepf, R. Bridging microscopes: 3D correlative light and scanning electron microscopy of complex biological structures. *Methods in Cell Biology* **111**, 325-356 (2012).
26. Koga, D., Kusumi, S., Bochimoto, H., Watanabe, T., Ushiki, T. Correlative light and scanning electron microscopy for observing the three-dimensional ultrastructure of membranous cell organelles in relation to their molecular components. *Journal of Histochemistry and Cytochemistry*. **63** (12), 968-979 (2015).
27. Peddie, C. J. et al. Correlative and integrated light and electron microscopy of in-resin GFP fluorescence, used to localise diacylglycerol in mammalian cells. *Ultramicroscopy*. **143**, 3-14 (2014).
28. Markert, S. M. et al. 3D subcellular localization with superresolution array tomography on ultrathin sections of various species. *Methods in Cell Biology*. **140**, 21-47 (2017).
29. Kolotuev, I., Schwab, Y., Labouesse, M. A precise and rapid mapping protocol for correlative light and electron microscopy of small invertebrate organisms. *Biology of the Cell*. **102** (2), 121-132 (2009).
30. Kolotuev, I. Positional correlative anatomy of invertebrate model organisms increases efficiency of TEM data production. *Microscopy and Microanalysis*. **20** (5), 1392-1403 (2014).

31. Schindelin, J. et al. Fiji: An open-source platform for biological-image analysis. *Nature Methods*. **9** (7), 676-682 (2012).
32. Miguel-Aliaga, I., Jasper, H., Lemaitre, B. Anatomy and physiology of the digestive tract of *Drosophila melanogaster*. *Genetics*. **210** (2), 357-396 (2018).
33. Nikolaev, M. et al. Homeostatic mini-intestines through scaffold-guided organoid morphogenesis. *Nature*. **585** (7826), 574-578 (2020).
34. Knoblich, J. A. Mechanisms of asymmetric stem cell division. *Cell*. **132** (4), 583-597 (2008).
35. Daniel, E. et al. Coordination of septate junctions assembly and completion of cytokinesis in proliferative epithelial tissues. *Current Biology*. **28** (9), 1380-1391 (2018).
36. Pasquettaz, R. et al. Peculiar protrusions along tanycyte processes face diverse neural and non-neural cell types in the hypothalamic parenchyma. *Journal of Comparative Neurology*. (2020).
37. Kremer, J. R., Mastronarde, D. N., McIntosh, J. R. Computer visualization of three-dimensional image data using IMOD. *Journal of Structural Biology*. **116** (1), 71-76 (1996).
38. Cardona, A. et al. TrakEM2 software for neural circuit reconstruction. *PLoS One*. **7** (6), e38011 (2012).
39. Belevich, I., Joensuu, M., Kumar, D., Vihinen, H., Jokitalo, E. Microscopy image browser: A platform for segmentation and analysis of multidimensional datasets. *PLoS Biology*. **14** (1), e1002340 (2016).

FIGURE 1

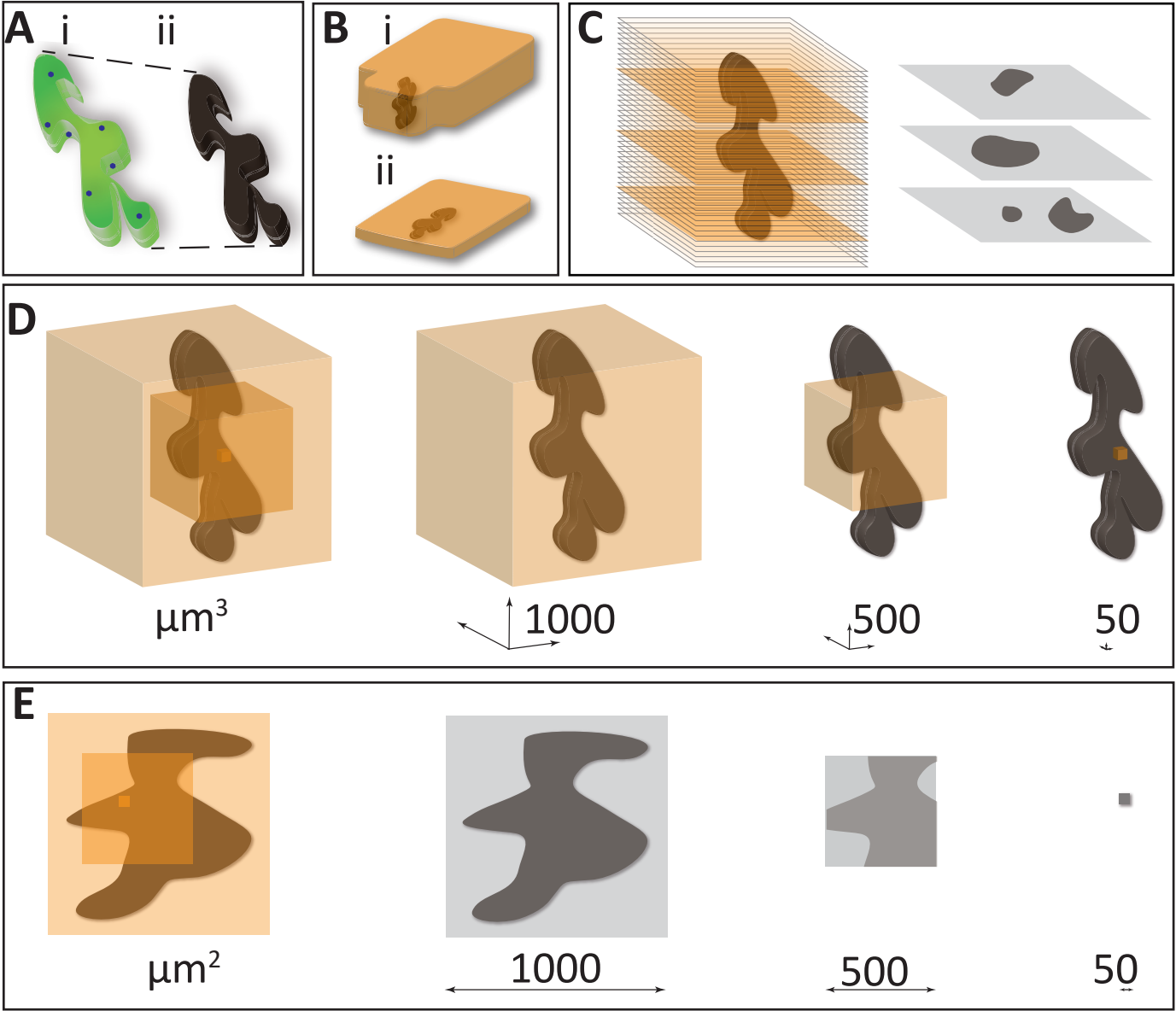


FIGURE 2

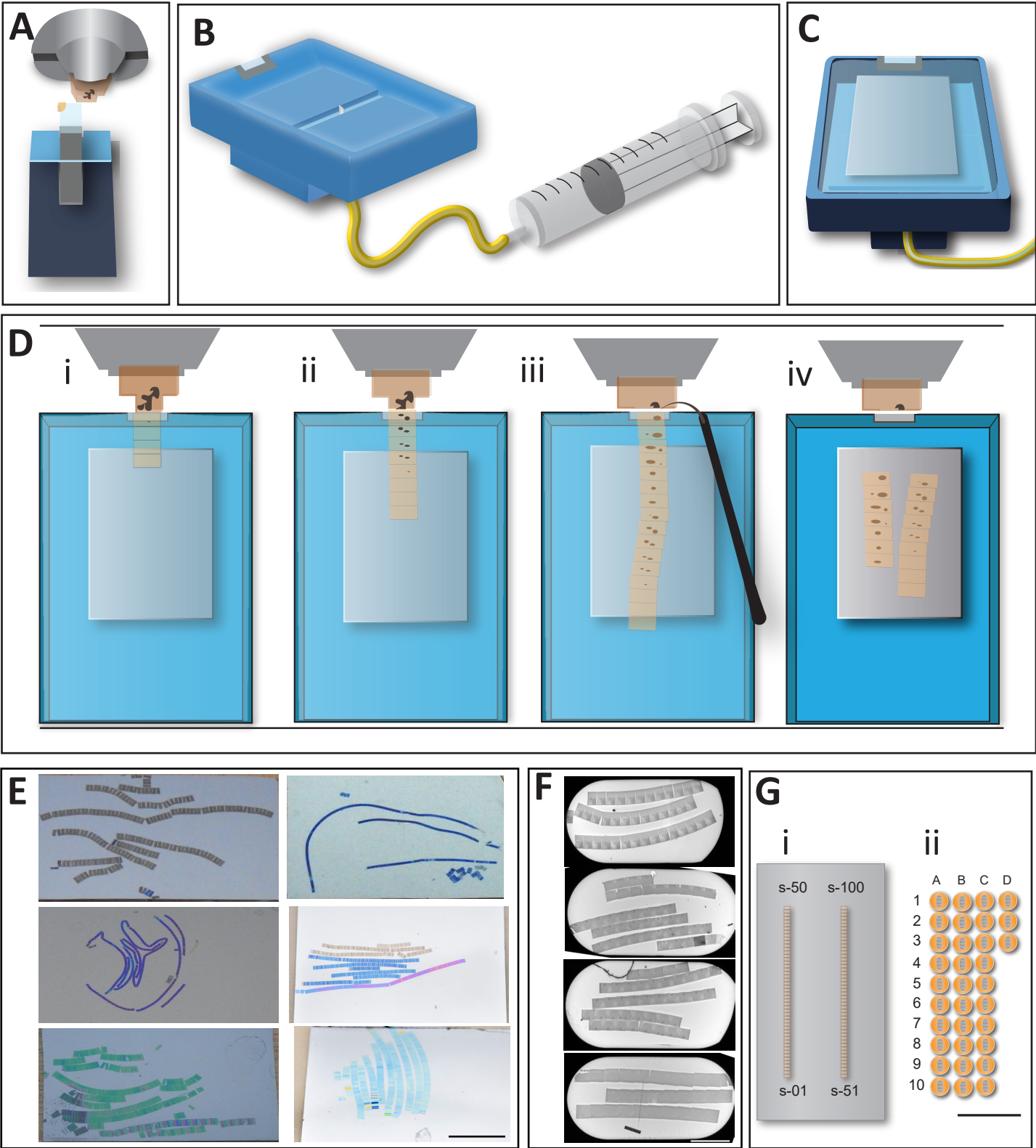


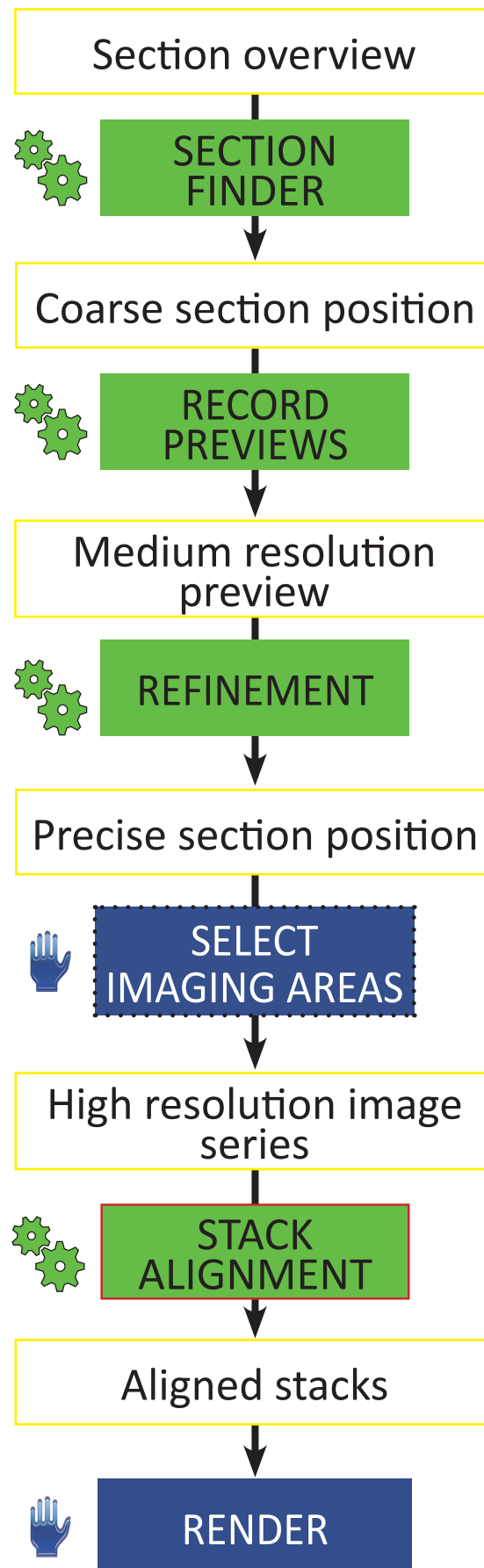
FIGURE 3

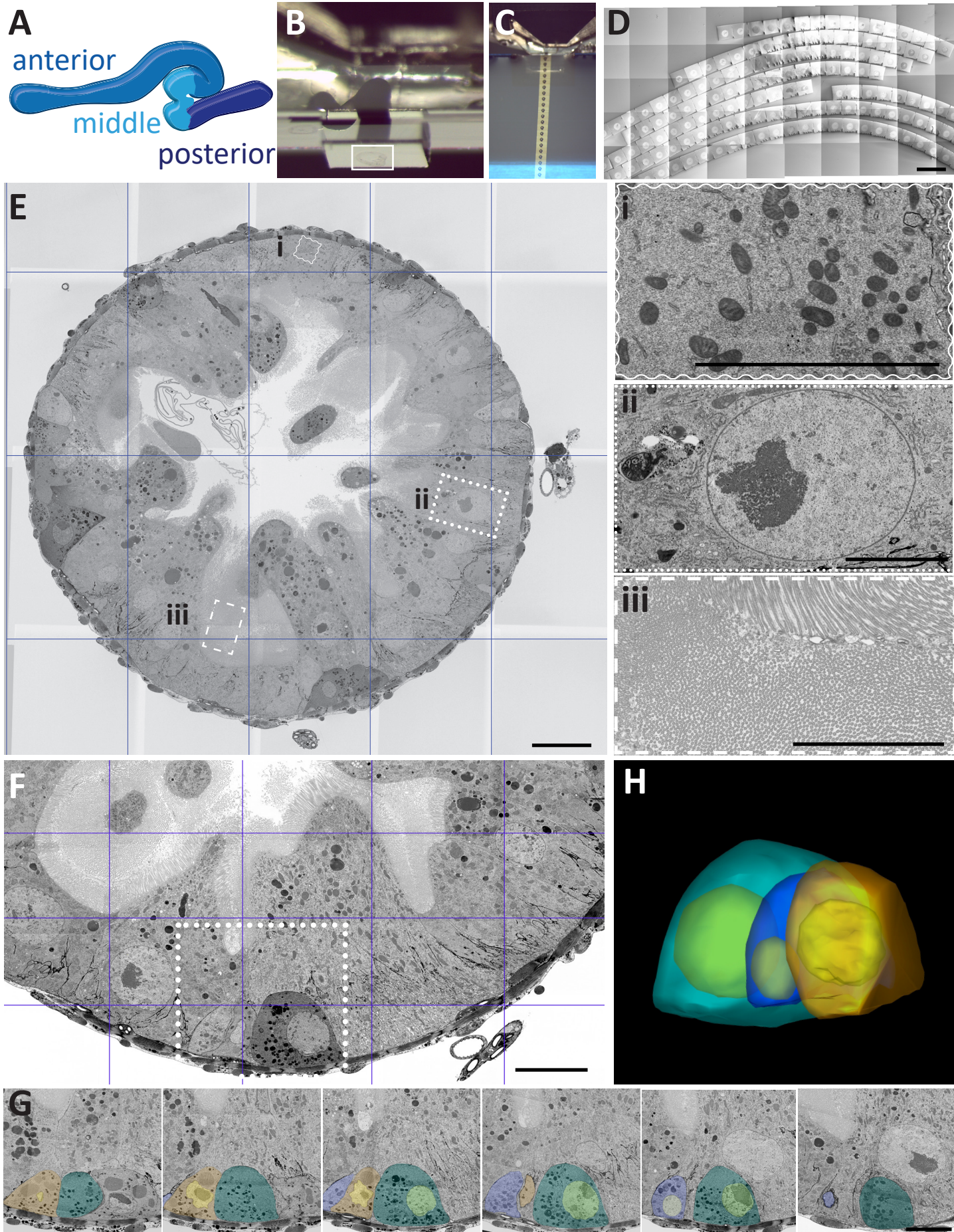
FIGURE 4

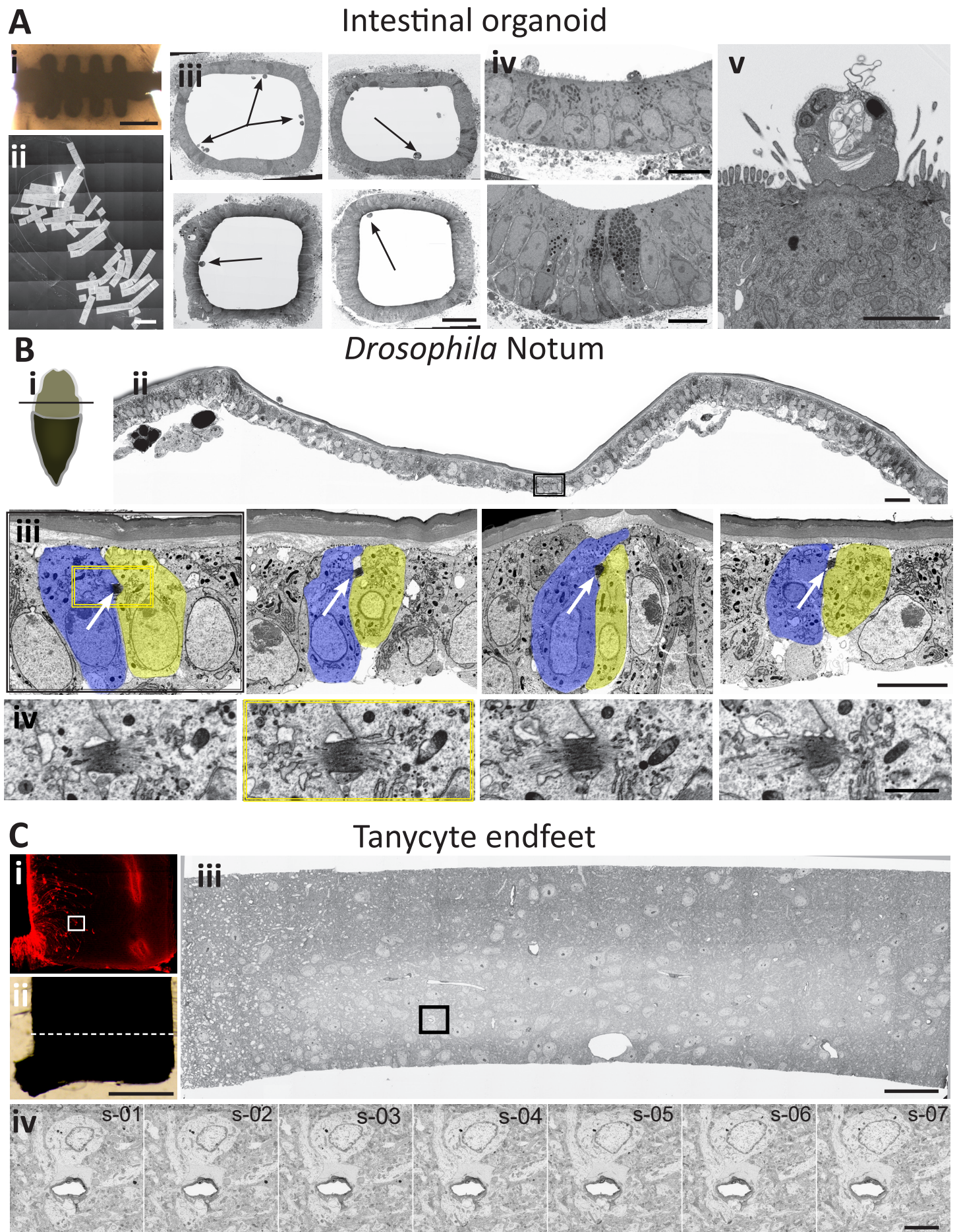
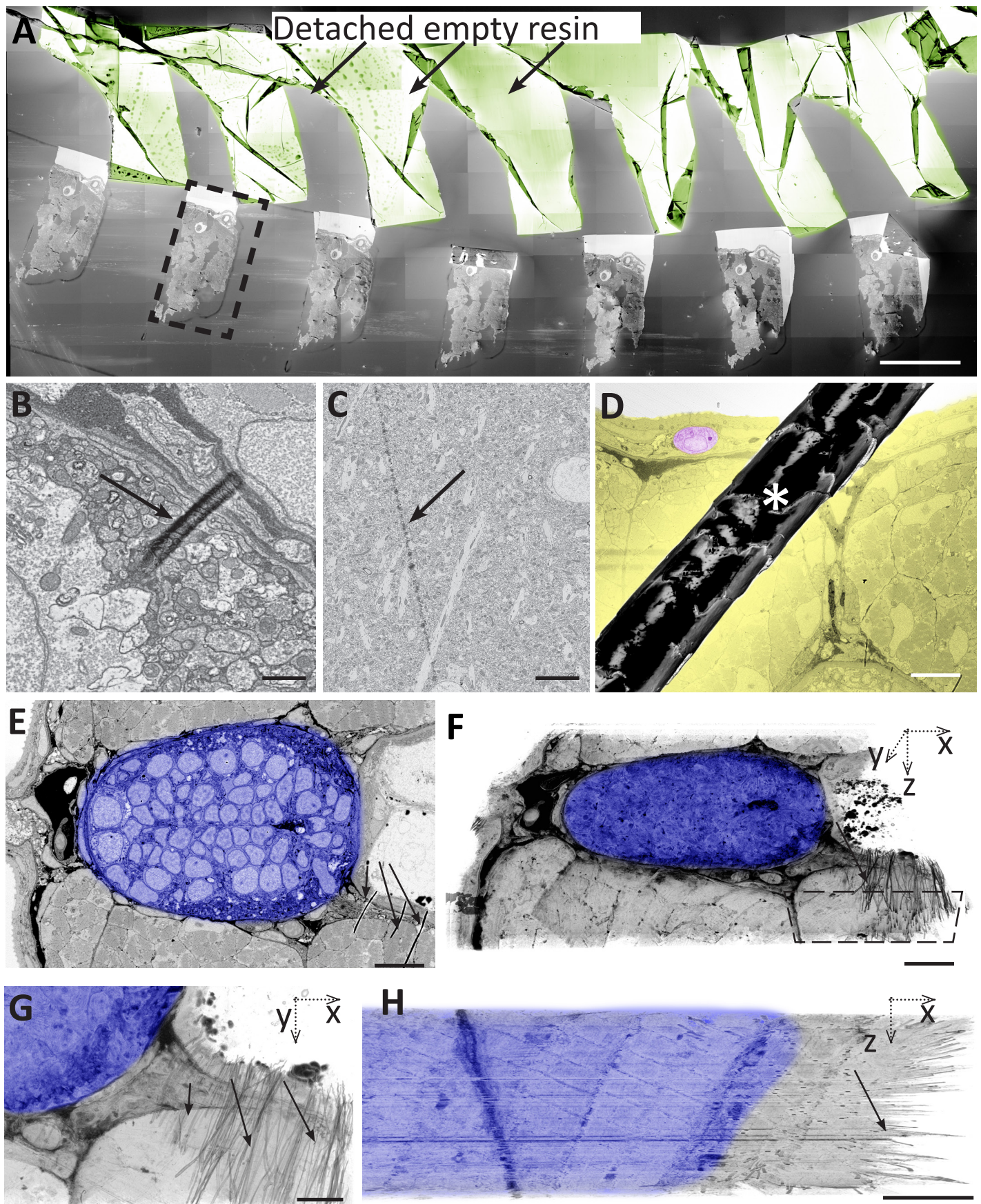
FIGURE 5

FIGURE 6

Name of Material/ Equipment	Company	Catalog Number
Cutting		
AT sectioning knife	Diatome	DUATS3530
Diamond knife for trimming 90°	Diatome	DTB90
Pattex contact adhesive	Pattex	PCL3C
Silicon wafer	Ted Pella	16015
Ultramicrotome	Leica UC6	
Wafer cleaving kit	EMS	7642
Image acquisition		
FESEM	Thermo Fischer Helios	1072419
Maps 3 for SEM with Correlative Workflow & Array Tomography	Thermo Fisher Scientific	1135932
Image analysis		
Amira x.y	Thermo Fisher Scientific	1131599
Image processing	Open source	Fiji (http://fiji.sc/#download)

Comments/Description
Diatome Jumbo knife
Diatome trimming 20°
Glass knife
Resistance: 1-30 Ohms
Type P: (Boron) (1 primary flat)
Roughness: 2 nm
No SiO2 top coating
TTV: = <20 µm
Wafer is polished on one side
Alternative: Leica UC7
EMF, Small Sample Cleaver, CatNo. 7652
an
Alternatives: Zeiss, Jeol, Hitachi, TESCAN
Maps provides automation of SEM imaging workflows and allows importing of 3rd party data for CLEM and navigation.
i
Amira is a 3D data visualization and analysis software with several practical functions for Array Tomography data reconstruction.
IMOD, MIB (See text for references)

Dear Vineeta,

Thanks a lot for clarifying over zoom different points we have raised. In this draft, we have addressed all the comments to the manuscript and hope that now the manuscript meets JOVE's publication criteria. Please, let us know if there is anything we still need to update.

Best regards,

Tilman and Irina

Supplementary methods

Workflow for SEM imaging on serial ultra sections in Maps

Tilman Franke and Irina Kolotuev

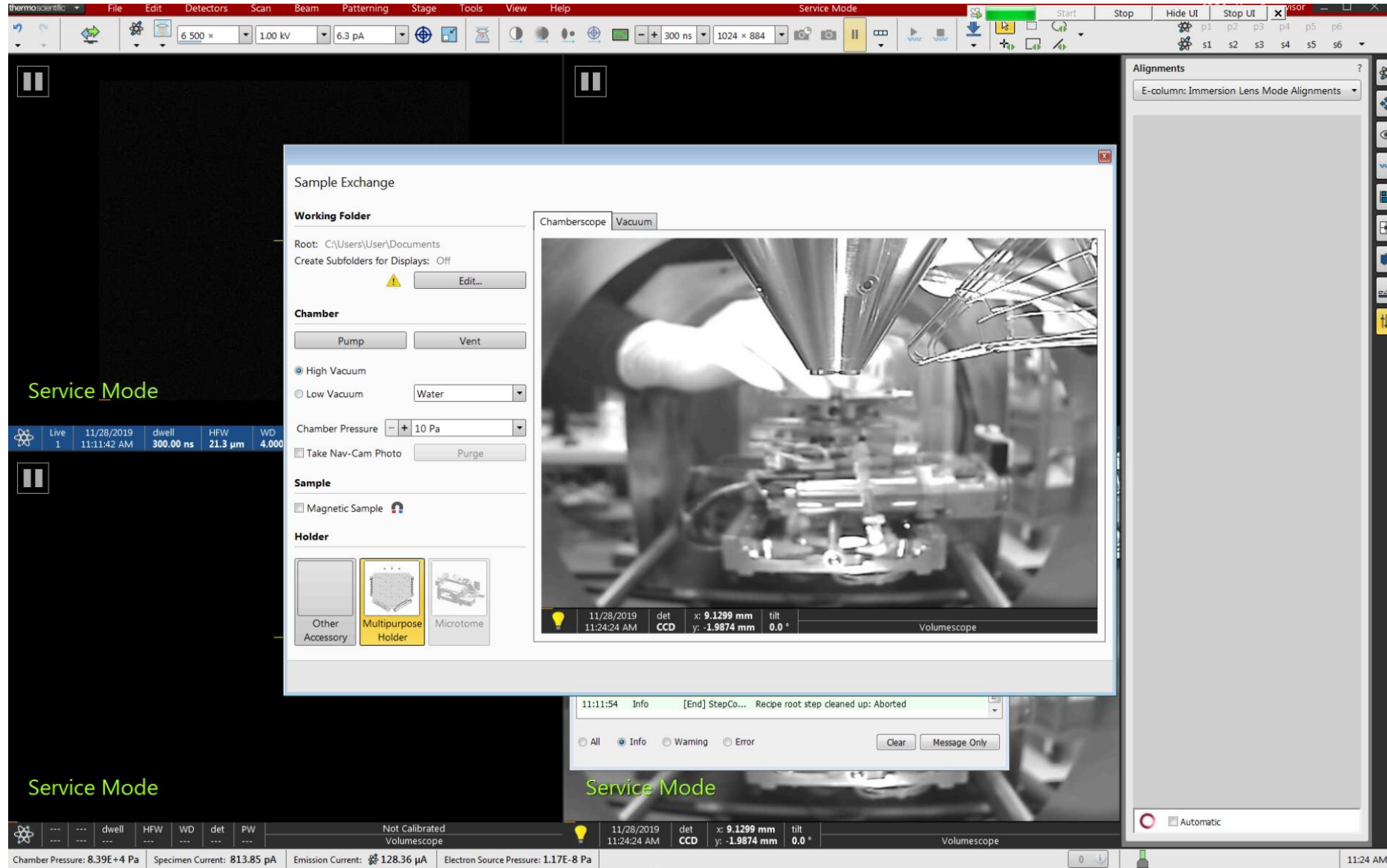
tilman.franke@thermofisher.com

irina.kolotueva@unil.ch

INDEX

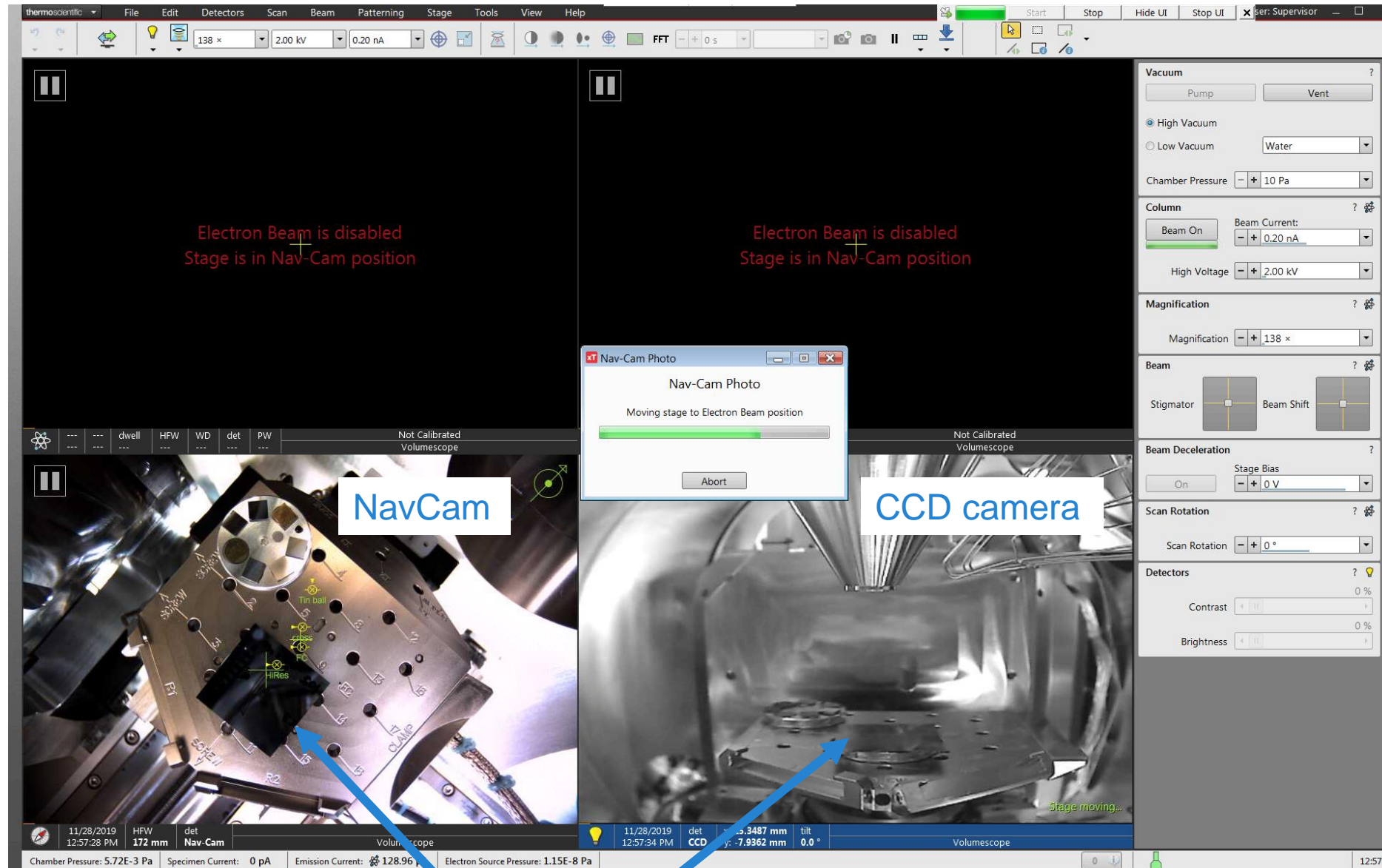
- Sample loading and NavCam usage *Page 2*
- SEM overview of the entire sample *Page 6*
- Determining the positions of all sections *Page 11*
- Acquisition of medium resolution overviews for position refinement and ROI identification *Page 16*
- Set up of unattended image acquisition with auto functions *Page 22*
- Troubleshooting and general advice *Page 26*

Sample loading



- The workflow starts with sample loading.
- Use the sample exchange dialog of the XT microscope control software to vent and open the vacuum chamber.
- Choose a suitable SEM holder to attach the Array Tomography sample and install it on the microscope stage.
- While closing the chamber door, observe the live camera view to make sure there is no collision with a detector.

Acquisition of Navigation image

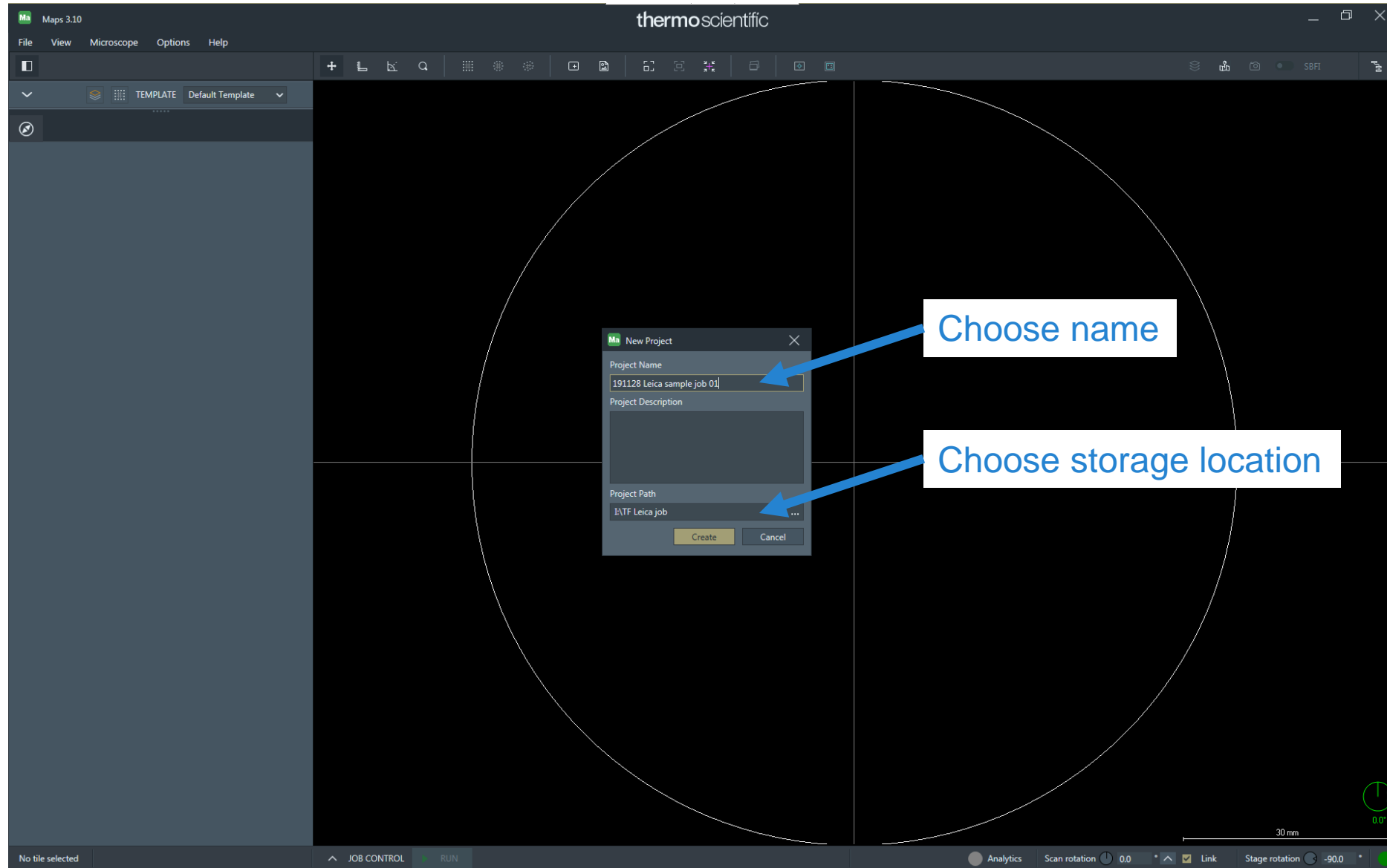


Most Thermo Fisher SEMs have two cameras. All systems are equipped with the “CCD camera” which looks at the sample from the side.

The optional NavCam is a color camera that can take a top down image of the sample holder and the sample.

- If available, acquire a NavCam image while pumping the vacuum. Alternatively, proceed to the next step.

New Maps project

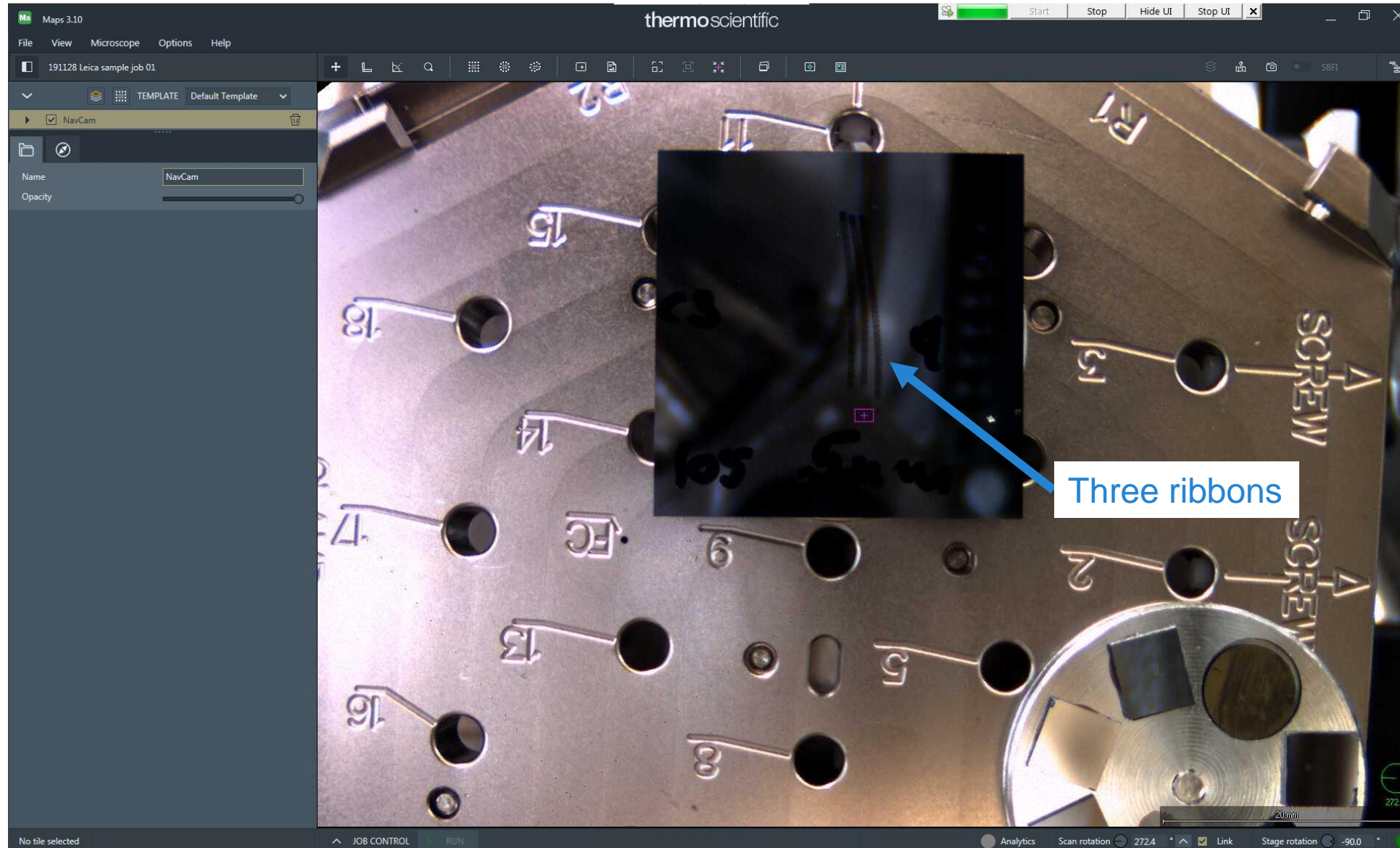


- Launch Maps software which runs alongside the XT microscope control software.

Maps has a zoomable viewer that shows any image recorded on a sample. Maps also automates workflows like tiling & stitching, CLEM, and array tomography.

- Directly after the start of the program, Maps asks the user to create a new Project. Do this by typing a project name and defining a storage location.

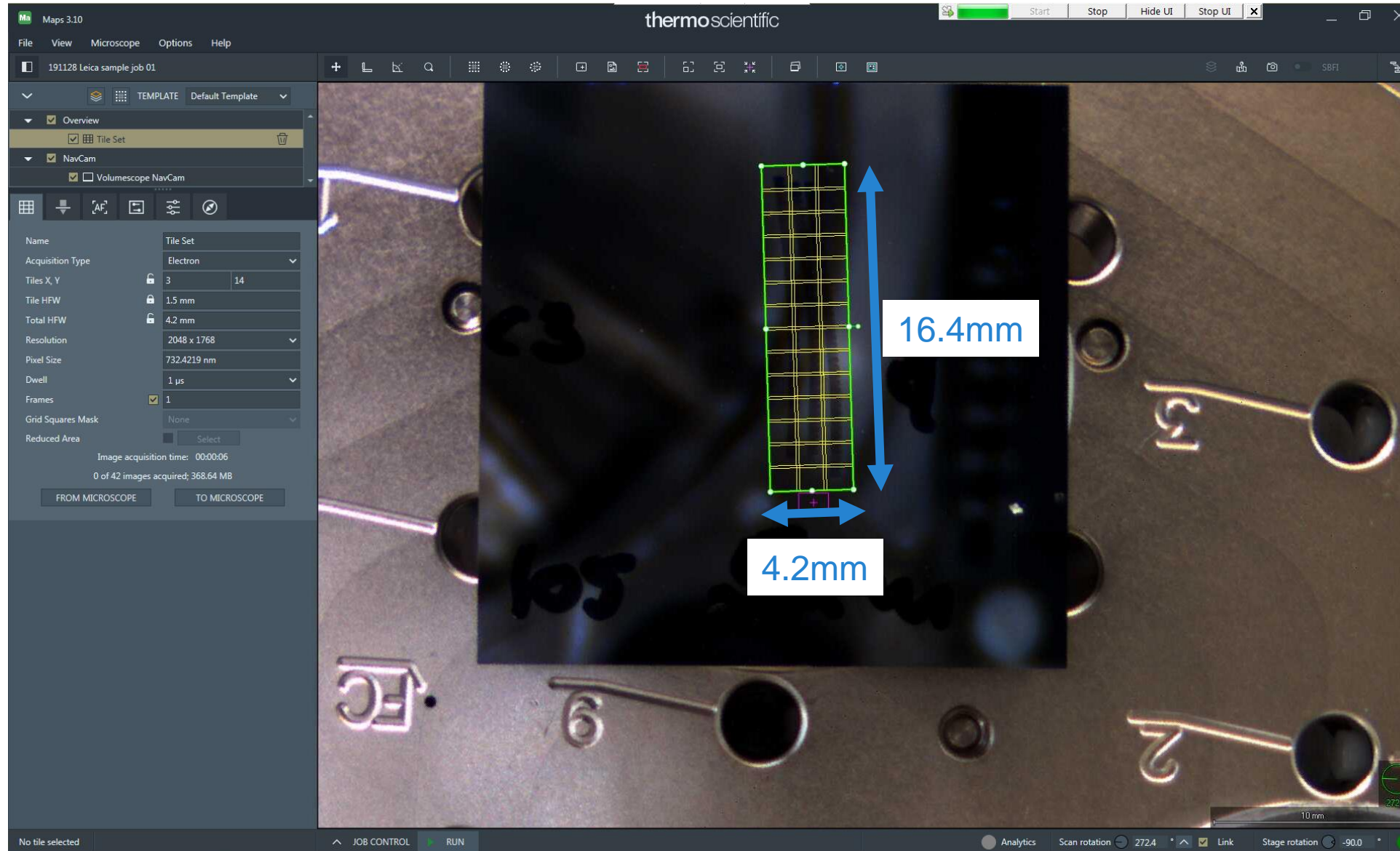
NavCam image in Maps



- Load the NavCam photo into Maps using the “Import from NavCam” feature in the Microscope menu.
- Zoom in until you can see the ribbons of sections on the silicon wafer.

The image quality is usually sufficient for the next step, which is positioning an SEM overview mosaic which will show the sections more clearly.

Creating an overview mosaic



- Create an image mosaic by drawing a rectangle while holding down the ALT key.
- Once created, the tiling layout can still be changed by dragging the corners of the mosaic.
- To fit the ribbons of sections optimally, it may be necessary to rotate the mosaic. To do this, grab and move the “lollipop” handle at the right-hand side of the mosaic.

Start acquisition - The job cue

The screenshot displays the Thermo Scientific Maps 3.10 software interface. The main window shows a large microscopy image of a sample with a grid overlay. On the left, the 'Overview' panel is visible, showing acquisition settings for 'Tile Set' and 'NavCam'. The 'Job Queue' panel is open, showing a list of jobs. The first job, 'Tile Set', is in progress, with a progress bar at 4% and a remaining time of 00:03:34. The 'RUN/STOP' button is highlighted with a blue arrow. The 'Job queue' label is also present, pointing to the job list. The 'Remaining time' label points to the time displayed at the bottom of the job queue panel.

thermoscientific

Maps 3.10

File View Microscope Options Help

191128 Leica sample job 01

TEMPLATE Default Template

Overview

Tile Set

NavCam

Volumescape NavCam

Name: Tile Set

Acquisition Type: Electron

Tiles X, Y: 3, 14

Tile HFW: 1.5 mm

Total HFW: 4.2 mm

Resolution: 2048 x 1768

Pixel Size: 732.4219 nm

Dwell: 1 μ s

Frames: 1

Grid Squares Mask: None

Reduced Area: Select

Image acquisition time: 00:00:06

1 of 42 images acquired; 368.64 MB

FROM MICROSCOPE TO MICROSCOPE

JOB QUEUE PROCESSING

DESELECT ALL SELECT ALL

Show completed jobs

Tile Set 4% Acquiring images... 00:03:34

POST ACQUISITION

Turn Off Beam When Done

React Detectors When Done

Sleep When Done

Pump to High Vacuum When Done

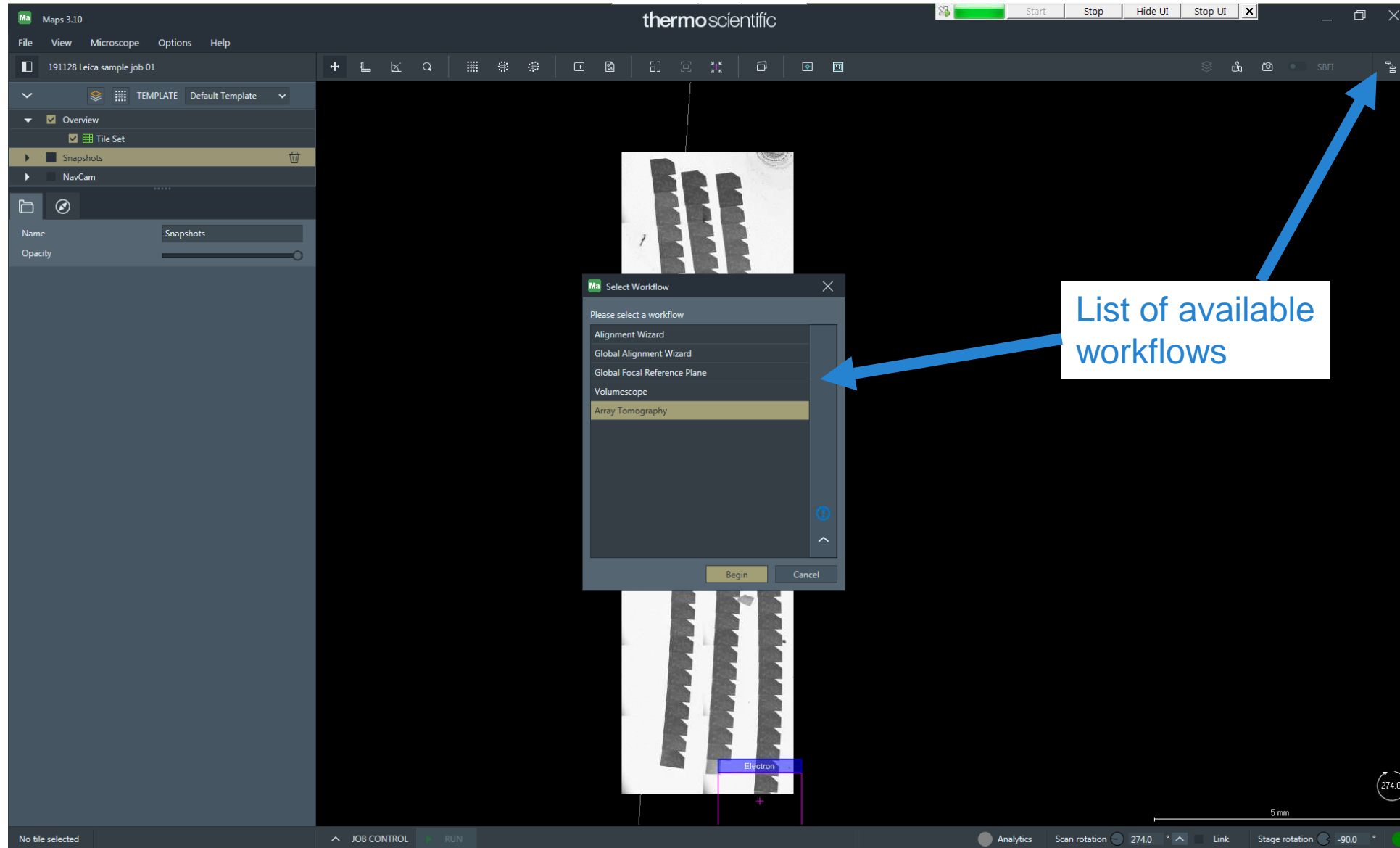
REMAINING TIME 00:03:34

Analytics Scan rotation 274.0 Link Stage rotation -90.0

Each added tile set appears in the job queue. After one tile set is finished, the next in queue will be launched automatically. The job queue also calculates the total time for all image recordings.

- Start recording by clicking the RUN/STOP button.

Starting the Array Tomo workflow

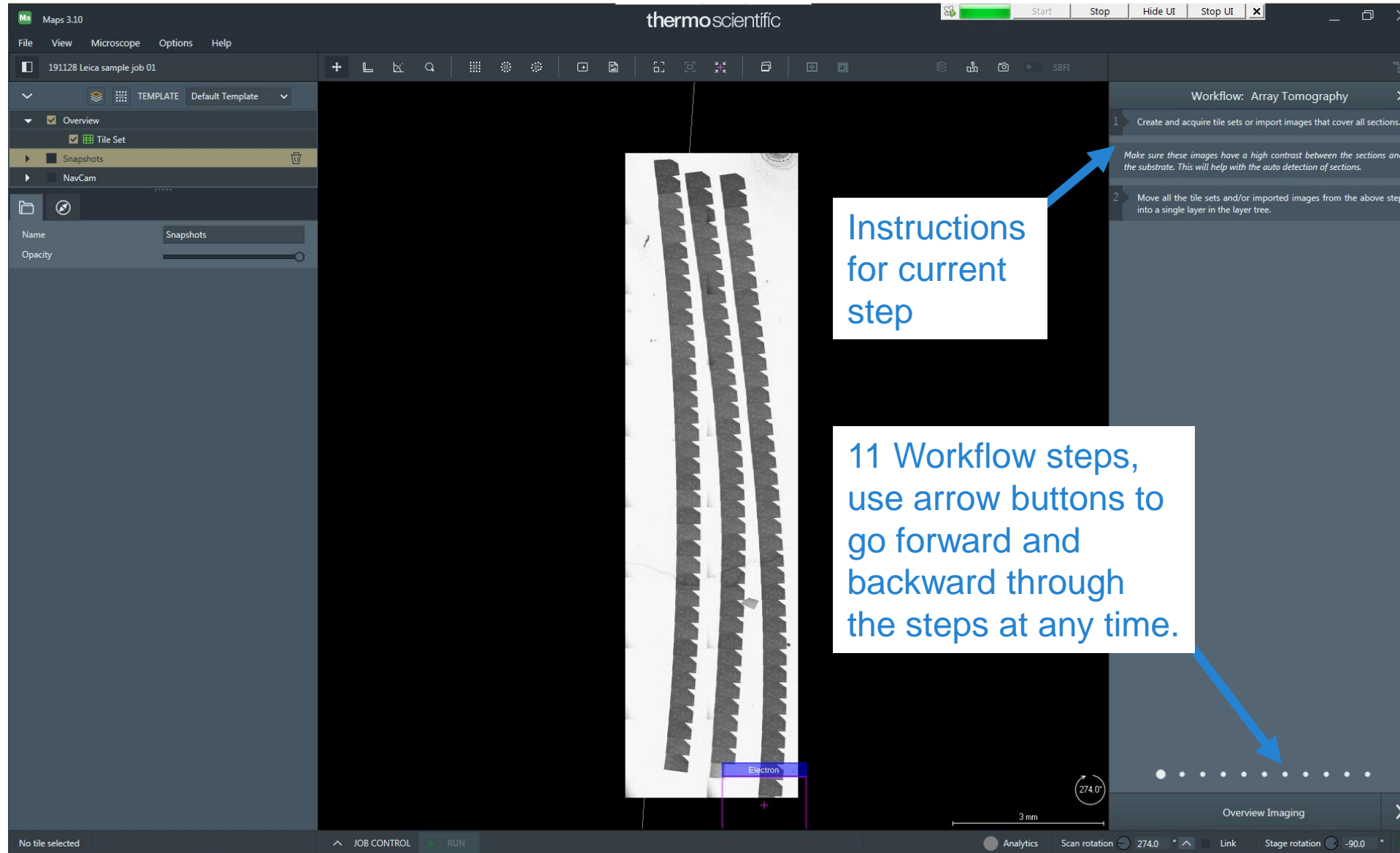


Once the SEM overview is recorded, one can hide the NavCam image.

The SEM overview mosaic shows the sections clear enough for the Automatic Section Finder.

- Launch the Array Tomography workflow by selecting it in the list.

The workflow panel

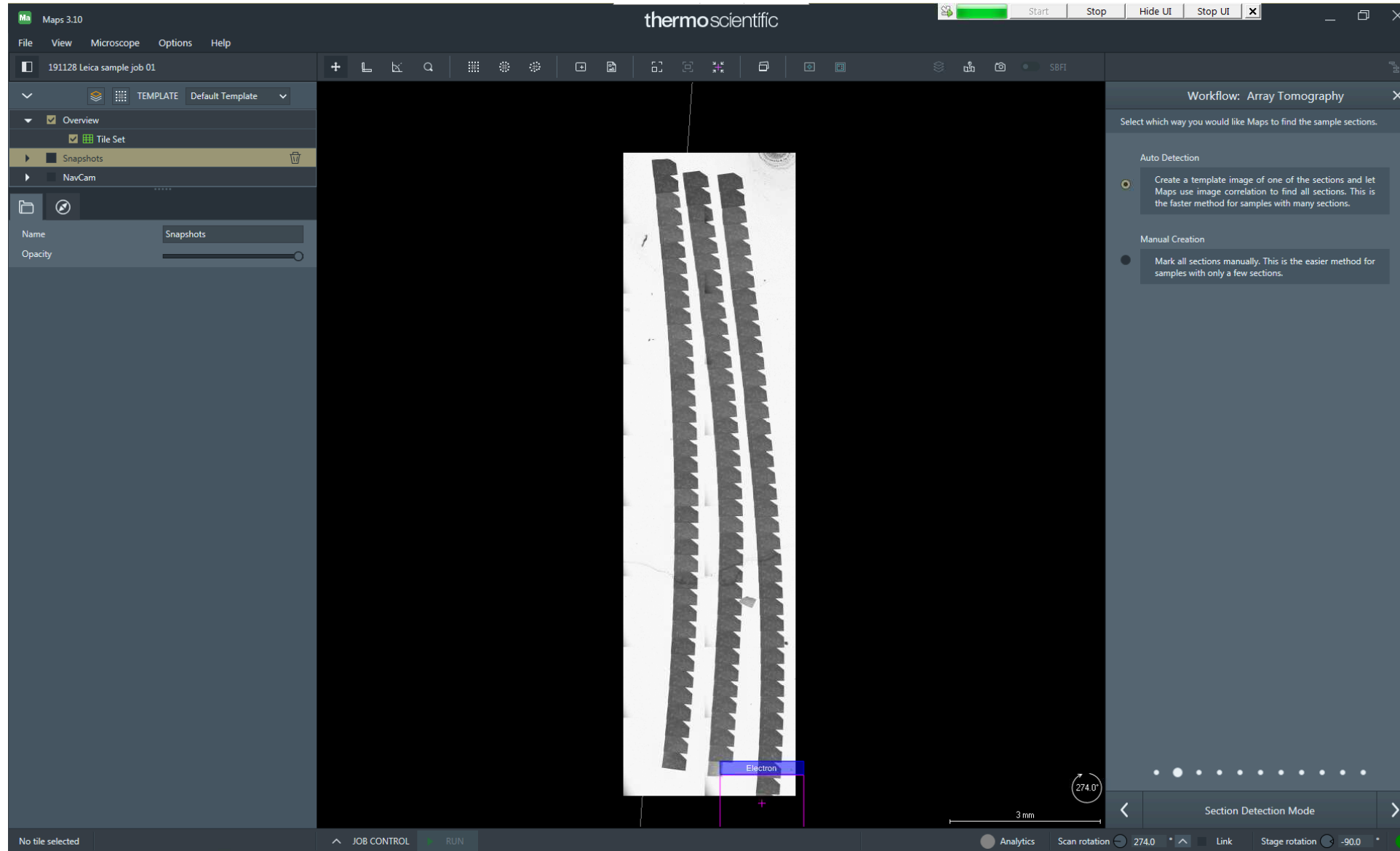


The Array Tomography Workflow consists of 11 steps, each represented by a Panel on the right-hand side of the screen.

- In each step, follow the instructions from top to bottom.

The first panel asks the user to acquire an SEM overview of the section set. As this was done already one can go directly to the next step.

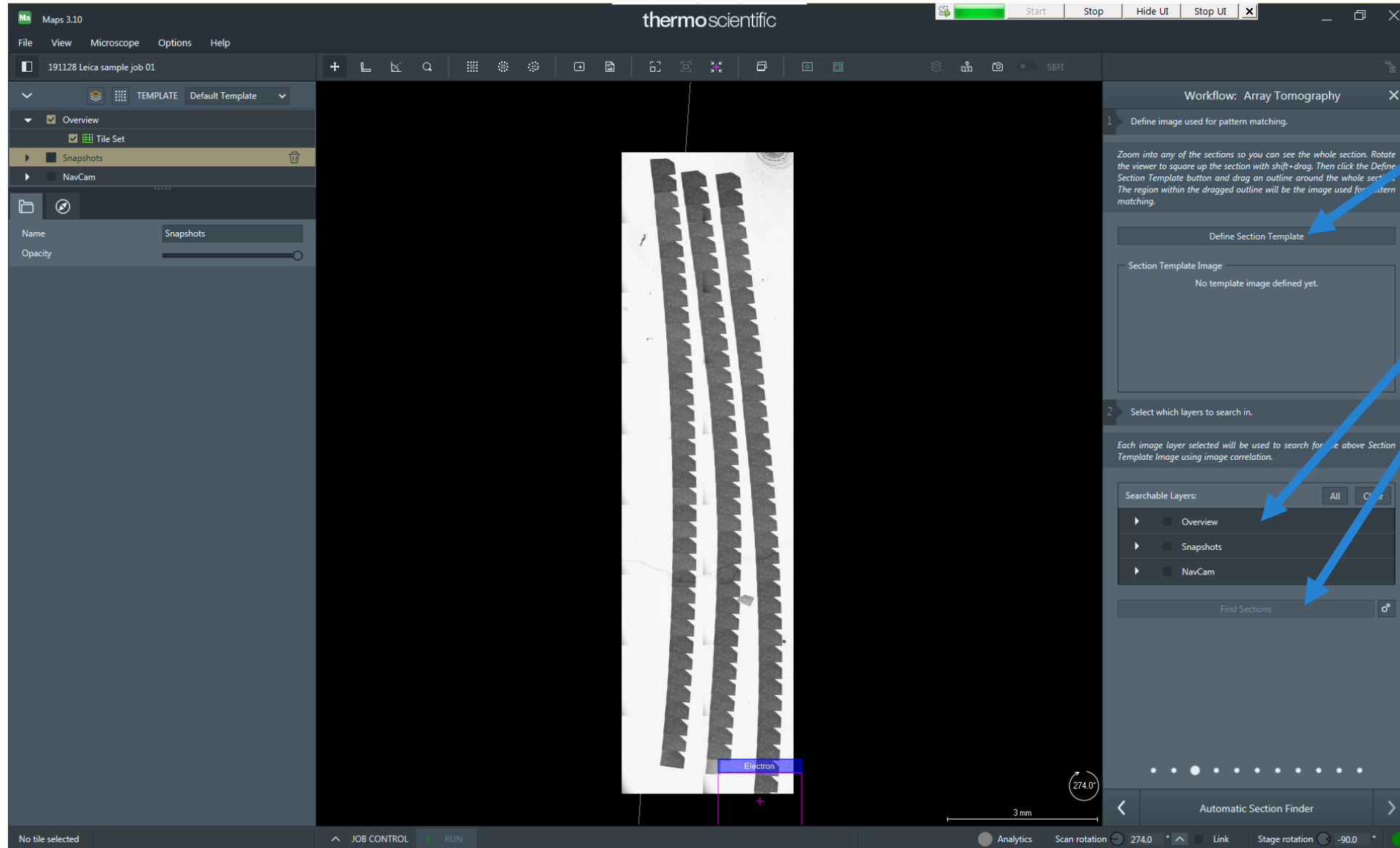
Step 2: Choose the Automatic Section Finder



In this step the user can decide between manual outlining of sections and the Automatic Section Finder.

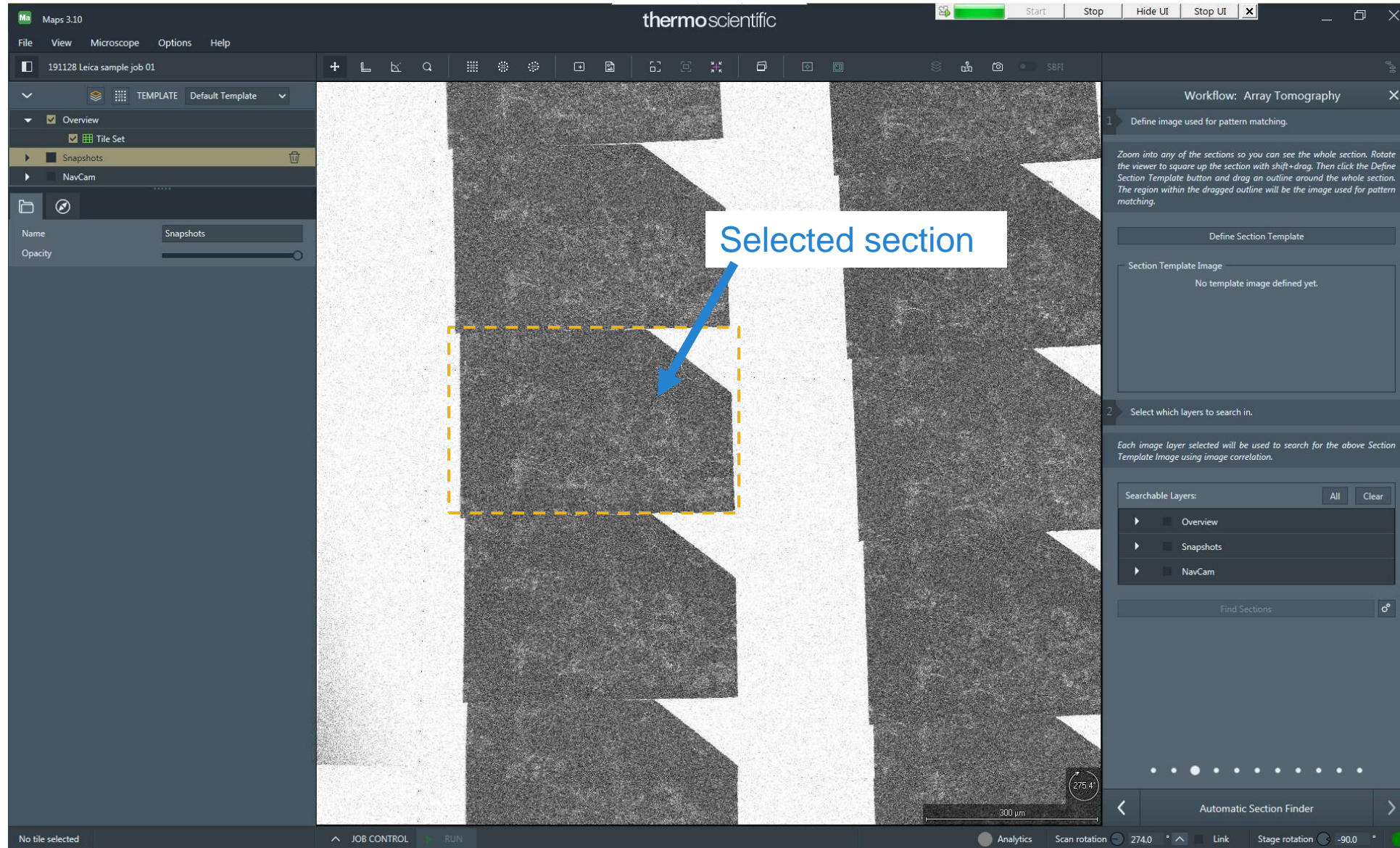
- Always choose „auto detection“!

Step 3: The Automatic Section Finder



- Zoom in on a section (any)
- Click „Define Section Template“
- Drag a rectangle around one of the sections (see also next slide)
- Select overview image(s) to search in
- Click „Find Sections“.

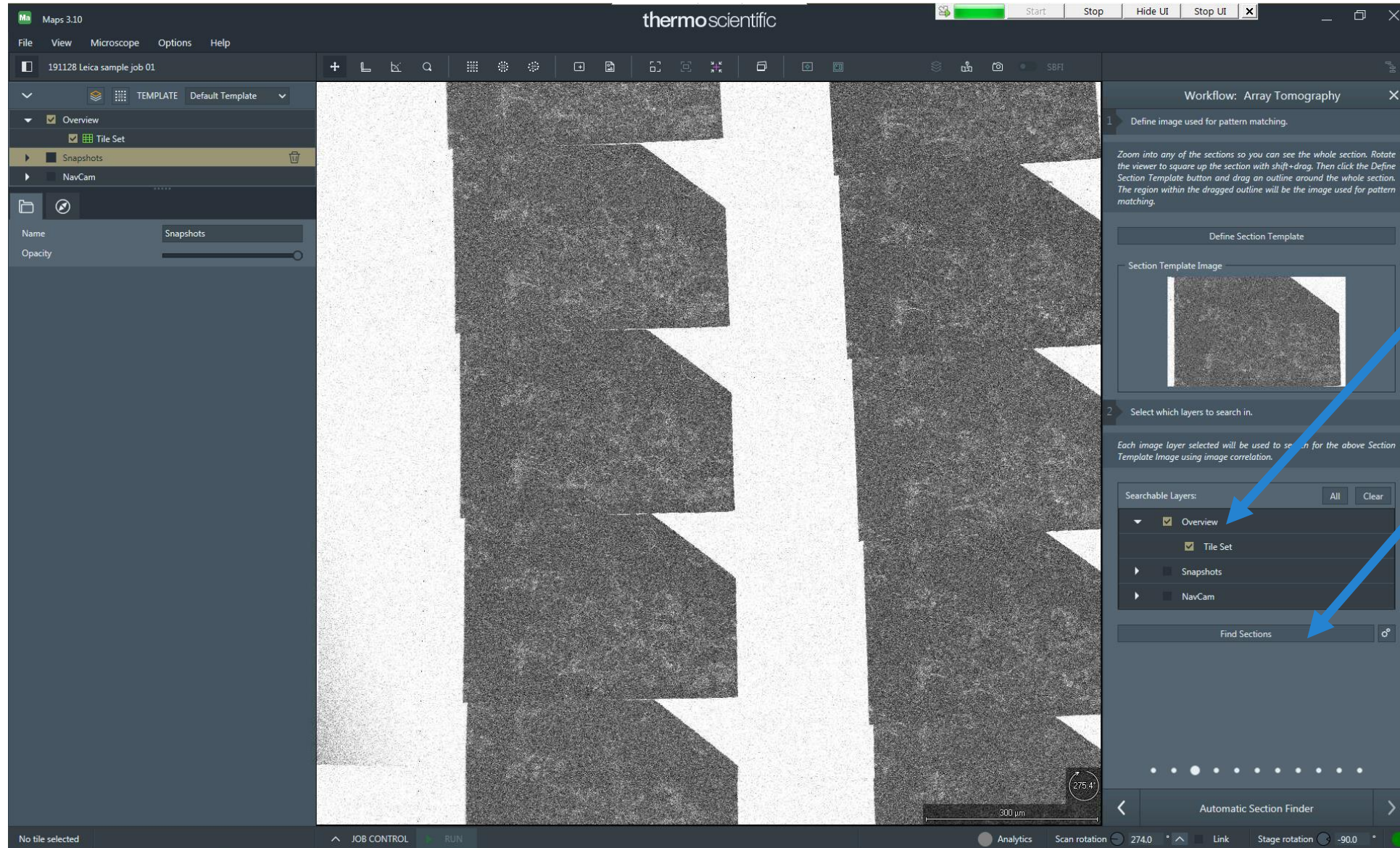
Step 3: The Automatic Section Finder



- Outline a section after zooming in by click+drag with the left mouse button.
- Choose a section in the middle of any of the ribbons.

Avoid sections with obvious artefacts (dust, folds).

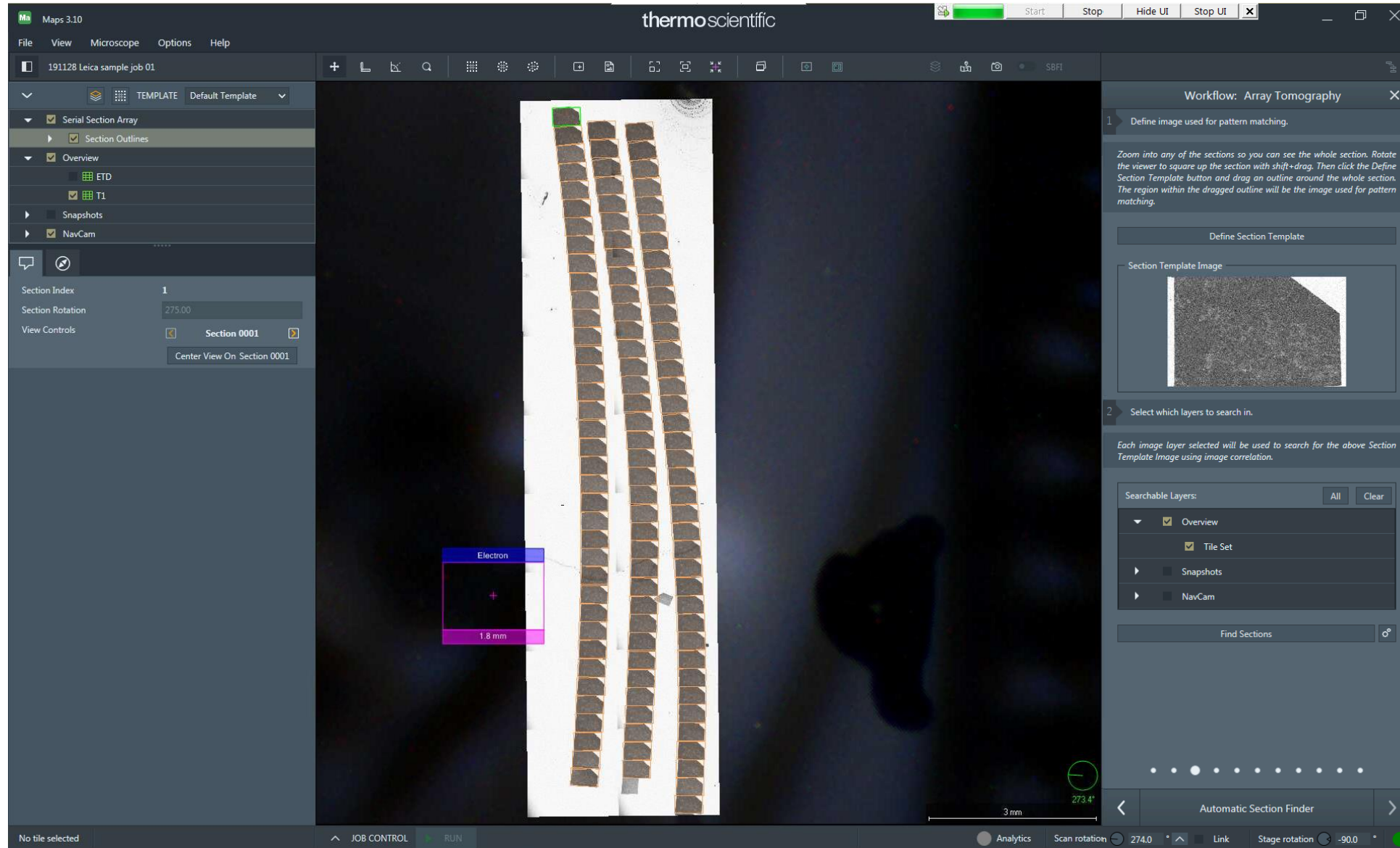
Step 3: The Automatic Section Finder



The outlined section is used as a search template which allows Maps to find all section positions.

- Check the boxes next to all images in which Maps should search for sections. It is possible to search in multiple overview mosaics at once!
- Click „Find Sections“.

Step 3: The Automatic Section Finder - Result

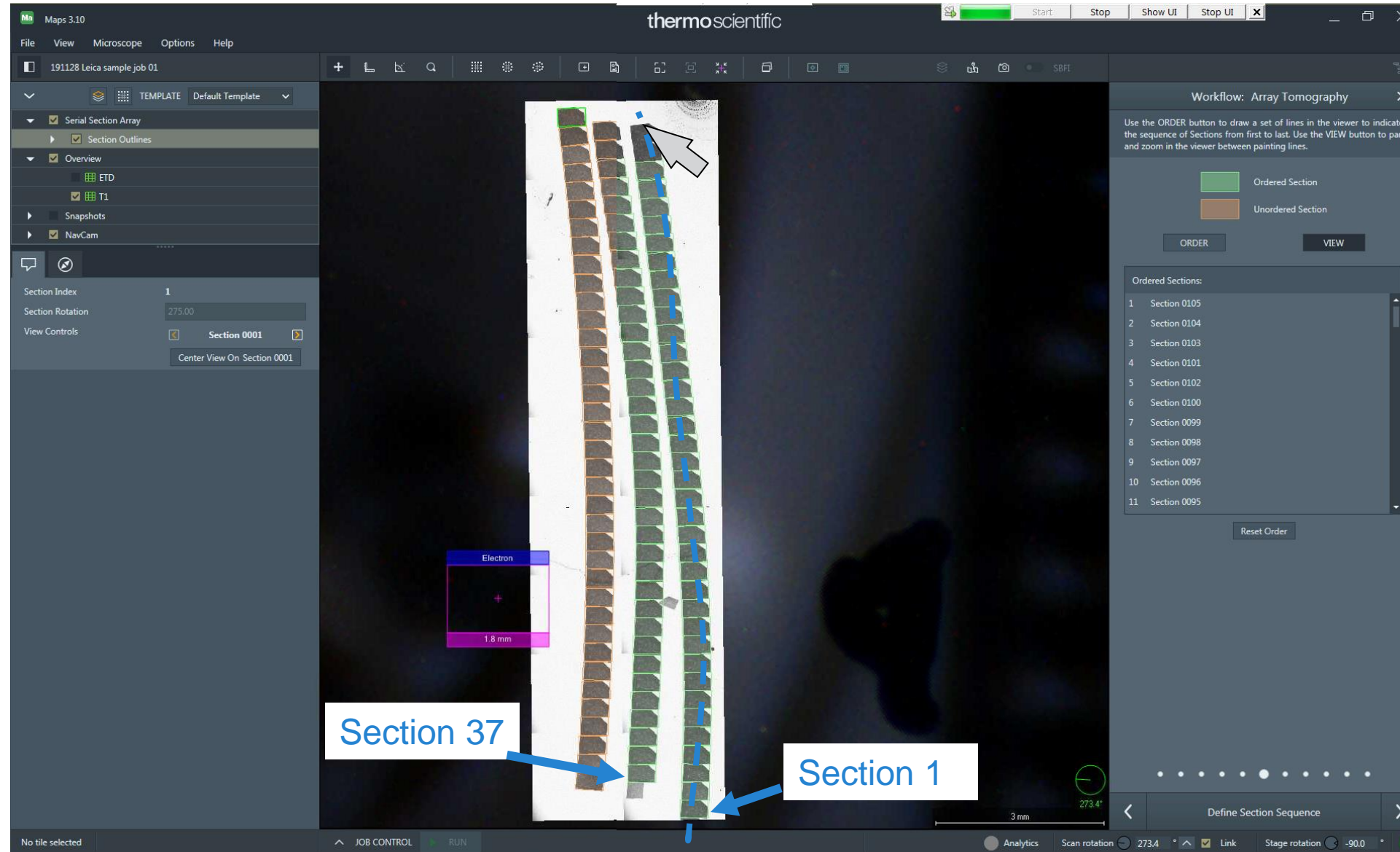


The Search usually takes 1-3min to complete. The quality of the recognition depends on the quality of the ribbons and type of the sample.

With tidy, high contrast samples as the one shown in this example the Finder usually does not miss sections and does not falsely detect other structures as sections.

In case not all sections are recognized correctly, one can manually add or remove sections or switch to the manual workflow and locate all sections manually (not shown here).

Step 6: Sort section sequence



(Steps 4 and 5 are not shown, as no sections needed to be added or removed.)

Sections are found in random order, so Maps needs the user to define their true sequence.

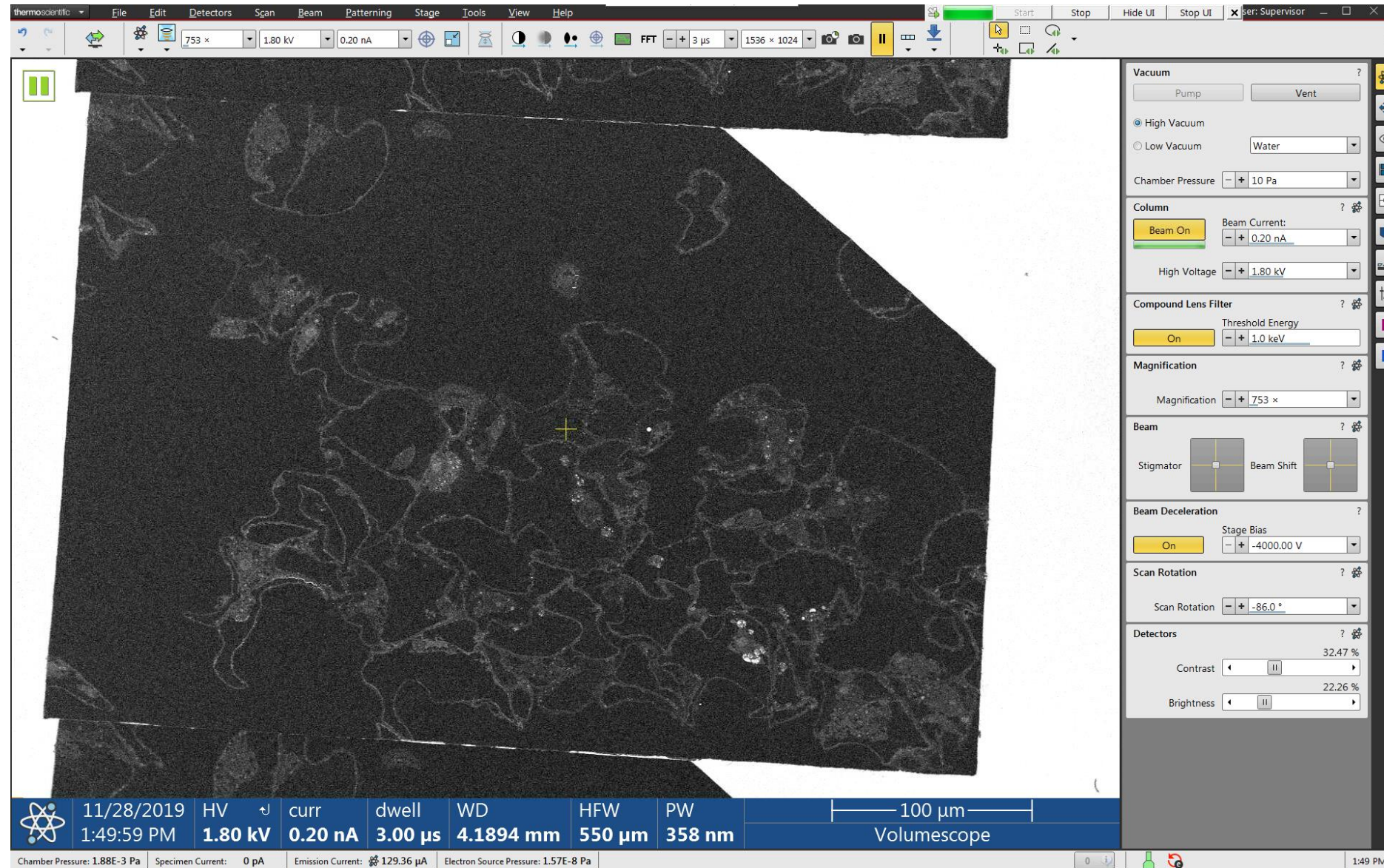
- Define the section sequence by clicking „ORDER“ and then drawing lines along the ribbons (left mouse click and drag).

The arranged sections turn green in the process.

Step 7: Record “Section Previews” - Rationale

- Section Previews are SEM images with higher resolution than the SEM overview. Typically, SEM overviews are acquired with a pixel size of 1-2 μ m, while Previews should average about 500nm per pixel. This increased resolution image set can be obtained within reasonable time as the software knows the section positions by now. Therefore, previews are only acquired on sections (one per section).
- Previews are needed in the following workflow steps for:
 - Navigation: The SEM overview mosaic is perfectly suitable for Section Finding but does not have high enough resolution for localizing areas of interest.
 - Image quality: Low signal-to-noise ratio is acceptable for overview mosaic and does not hinder the success rate of the Section Finder. Preview images, however, should be less noisy, as they will be used by the operator for locating ROIs. As Preview images are recorded in a much smaller total area (only on sections, not the empty space in between), it is possible to increase the pixel dwell time (for example from 1 μ s to 3 μ s) while maintaining an acceptable recording time.
 - Precision: Image mosaics can have discontinuities on tile borders, especially if the tiles are large. Preview images, on the other hand, are acquired without tiling. Each Preview is centered on one section. This minimizes the impact of geometric imperfections that SEMs can have in large fields of view.
 - Position Refinement: Section Previews are the basis for the Position Refinement step, which follows in the workflow.

Step 7: Find good imaging settings for Section Previews



- Use live imaging in the XT software to find good imaging parameters and to adjust contrast and brightness.

These parameters are typically used:

- 1.5-2kV
- 100-800pA
- 4mm working distance
- 1-3µs pixel dwell time
- Field size sufficient to contain one section
- Pixel size ~500nm

Step 7: Record all Preview images

The screenshot shows the Thermo Scientific Maps 3.11 software interface. The main window displays a grid of section previews, with yellow frames highlighting the regions to be acquired. A blue arrow points to these frames with the text: "Yellow Frames mark yet-to-be-acquired imaging regions." The left sidebar shows a list of section previews, with "Section 0001-preview" selected. The bottom panel shows the "Workflow: Array Tomography" panel, which includes instructions for acquiring section previews and buttons for "Go To First Section", "Acquire First Section Preview", and "Acquire All Section Previews".

Workflow: Array Tomography

In this step, high resolution images will be acquired at each section which will be used to increase the accuracy of the section outline placement in the next step.

- 1 Use the Go To First Section button to bring the viewer and stage to the first Section.
- 2 Use the microscope UI to set up suitable acquisition settings and click the Acquire First Section Preview button to create and acquire first preview image using these settings.
- 3 Use the Acquire All Section Previews button to have Maps record previews of all Sections.

Tips: Try and encompass the whole section in the field of view if possible. This will reduce acquisition time. Make sure you can see a good contrast of details within the section. Make sure the sample is in focus. Try to have at least 2k resolution. These tips will all help for the refinement in the next step.

Make sure the first section preview is in focus and has visible sample details. The Acquire All Section Previews button will create and acquire an identical tile set as the first preview on the rest of the sections.

Buttons: Go To First Section, Acquire First Section Preview, Acquire All Section Previews, Acquiring Section Previews..., Reset Previews.

Section Previews (optional)

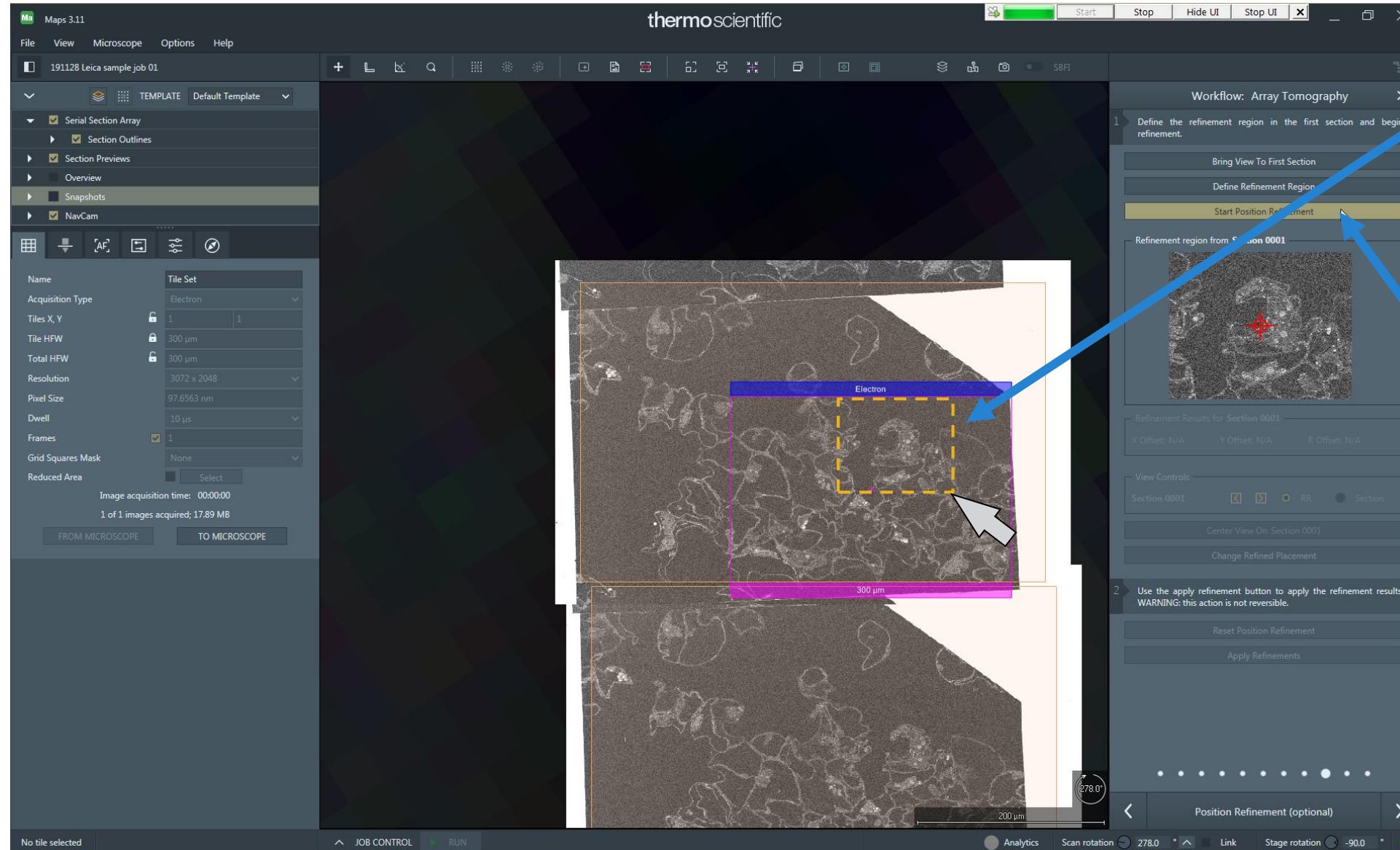
Job Control: STOP, REMAINING TIME: 00:00:01

- Back in Maps, click three buttons:
- „Go To First Section“, which moves the stage and the Maps viewer to the first section,
- „Acquire First Section Preview“, which gives the user a chance to review the imaging settings before acquiring all remaining Previews.
- „Acquire All“.

Step 8: Position Refinement - Rationale

- Ultimately, we want to outline an imaging region in (any) one section, clone it to exactly the same relative location in all sections, and record the data as an image stack. We want all images to be well aligned.
- In reality this is very hard: Stage precision of $\pm 1\mu\text{m}$, geometric distortions of the images, and variability of the sections themselves (stretching, compression, folds) cause at least $10\mu\text{m}$, often $100\mu\text{m}$ of variability of imaging region placement.
- Position Refinement is a function that reduces the position variability of imaging regions.
- It allows the user to select a local area in one of the Section Previews, which is then used by Maps as a search template. This template is matched in all the Section Preview images (it is also periodically updated in the process). From the matching positions, offsets are determined which are then used to improve imaging region placement.
- In case of variable compression/distortion, the correction is most precise in and around the selected template area. For acquisition of images in other, far away areas, it is possible to run Refinement a second time.

Step 9: Position Refinement



- Zoom in on the first section and outline an area around one or several regions of interest (left mouse button).

The template is shown in the workflow panel.

- Click „Start position Refinement“.

Step 9: Position Refinement

Updating template shown here

Section outlines turn green once their position has been refined.

Workflow: Array Tomography

1 Define the refinement region in the first section and begin refinement.

Bring View To First Section

Define Refinement Region

Start Position Refinement

Refinement region from Section 0093

Performing refinement on Section 0094

Progress:

Refinement Results for Section 0093

X Offset: -7.3676 μm Y Offset: -9.6741 μm R Offset: -2.33°

Stop Refinement

2 Use the apply refinement button to apply the refinement results. WARNING: this action is not reversible.

Reset Position Refinement

Apply Refinements

Position Refinement (optional)

No tile selected

JOB CONTROL RUN

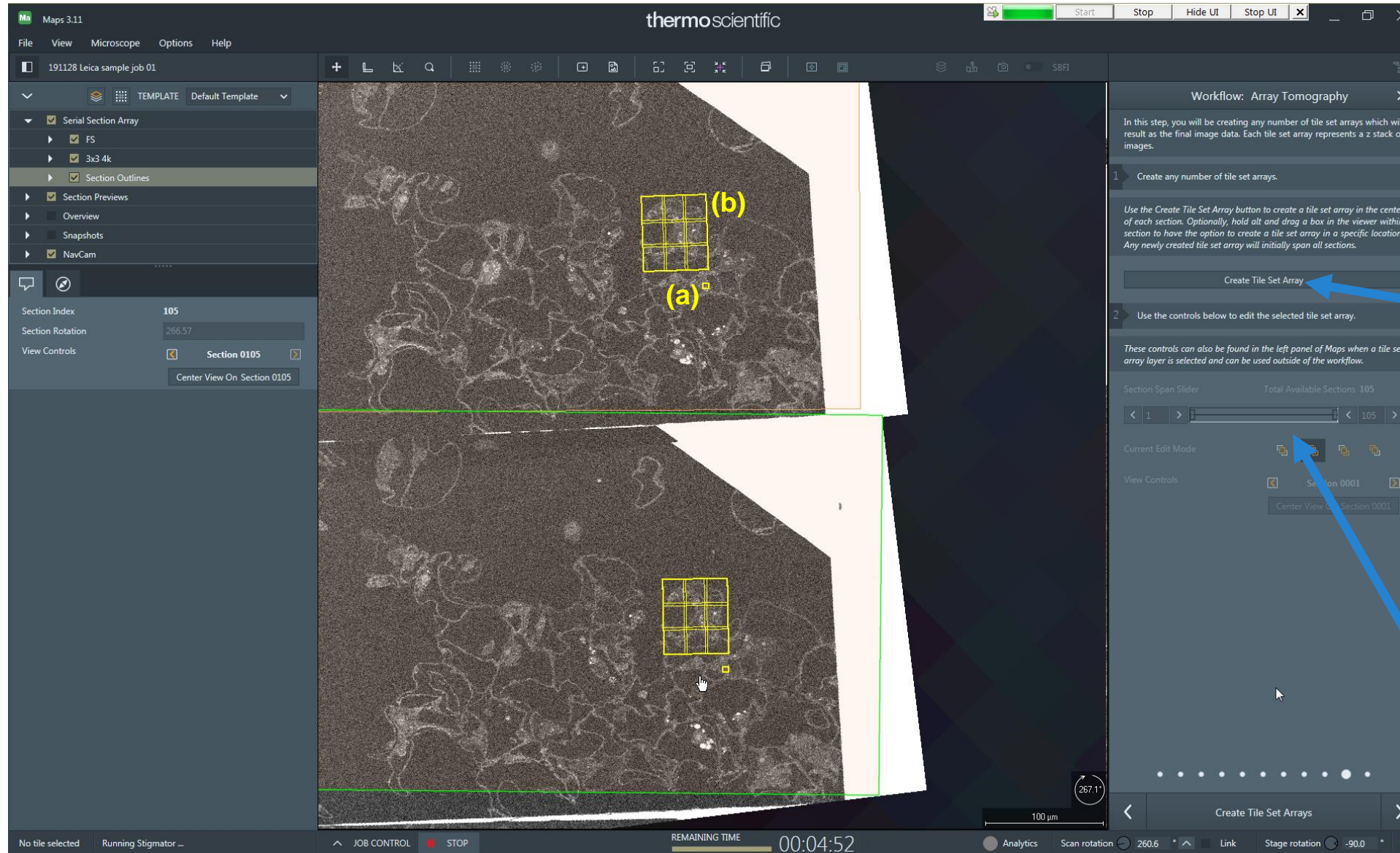
Analytics Scan rotation 278.0° Link Stage rotation -90.0°

- Observe the updating template while the refinement is continuing through the section set: there should not be jumps or drift.
- In case of failure, choose larger search template.

The process takes approximately 2 minutes.

If it fails consistently, in 99% of cases the section sequence is not correct! A jump (missing sections) or a mix-up in the section sequence can make it impossible to find a match.

Step 10: Create “Array Tile Sets”: Imaging regions that are cloned to all sections



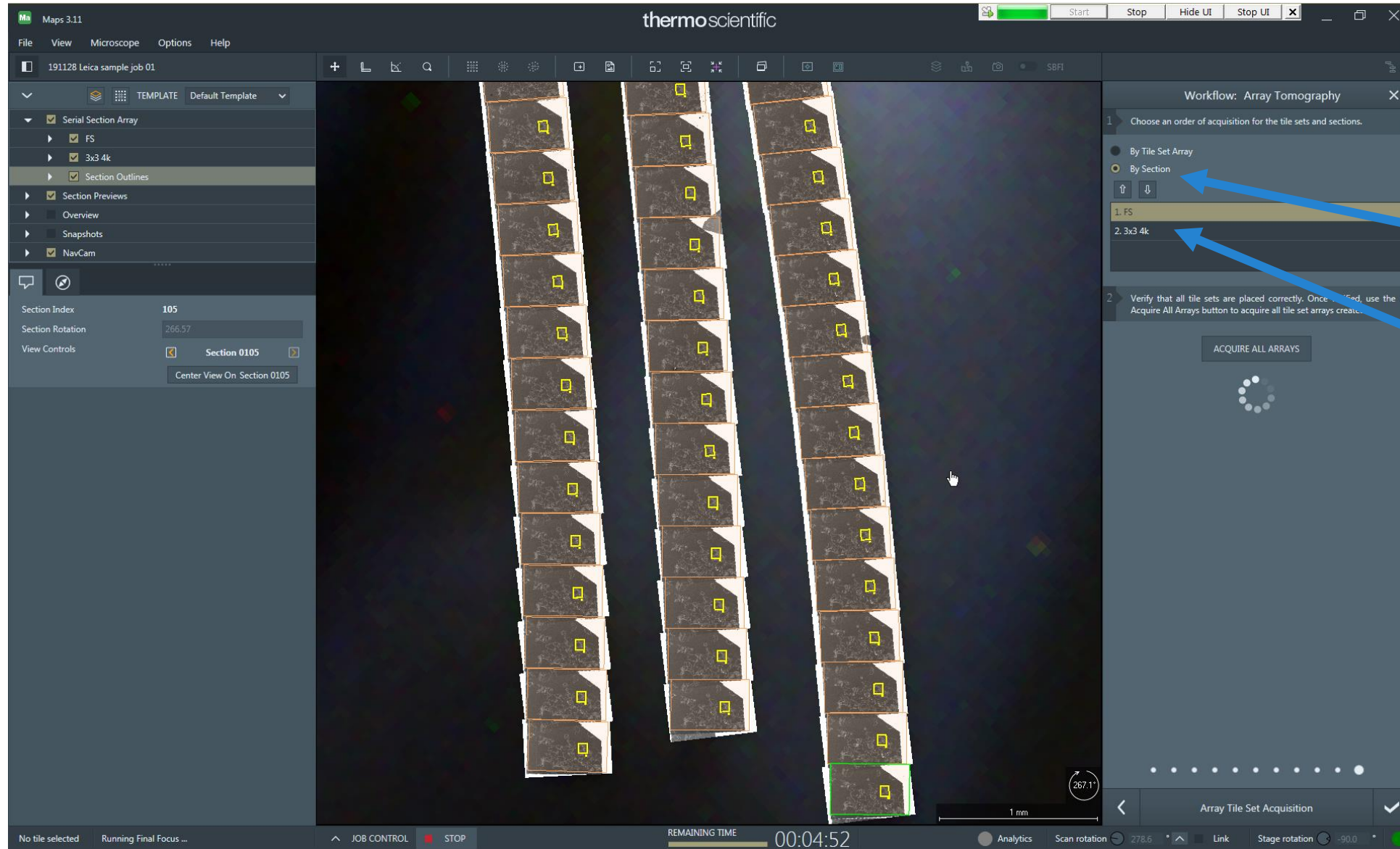
Multiple different Array Tile Sets can be set up, each with individual size, position, rotation, and imaging settings (including mosaics).

- Create one or several Array Tile Sets (imaging regions which are repeated on many or all sections) using the button in the panel.

Position, rotation, and imaging parameters can be changed at any time; changed parameters are always cloned to all images that constitute the series.

- Define start and end section for each Tile Set using the Section Span Slider (default: tile set will be recorded on all sections).

Step 11: “Acquire all arrays”!



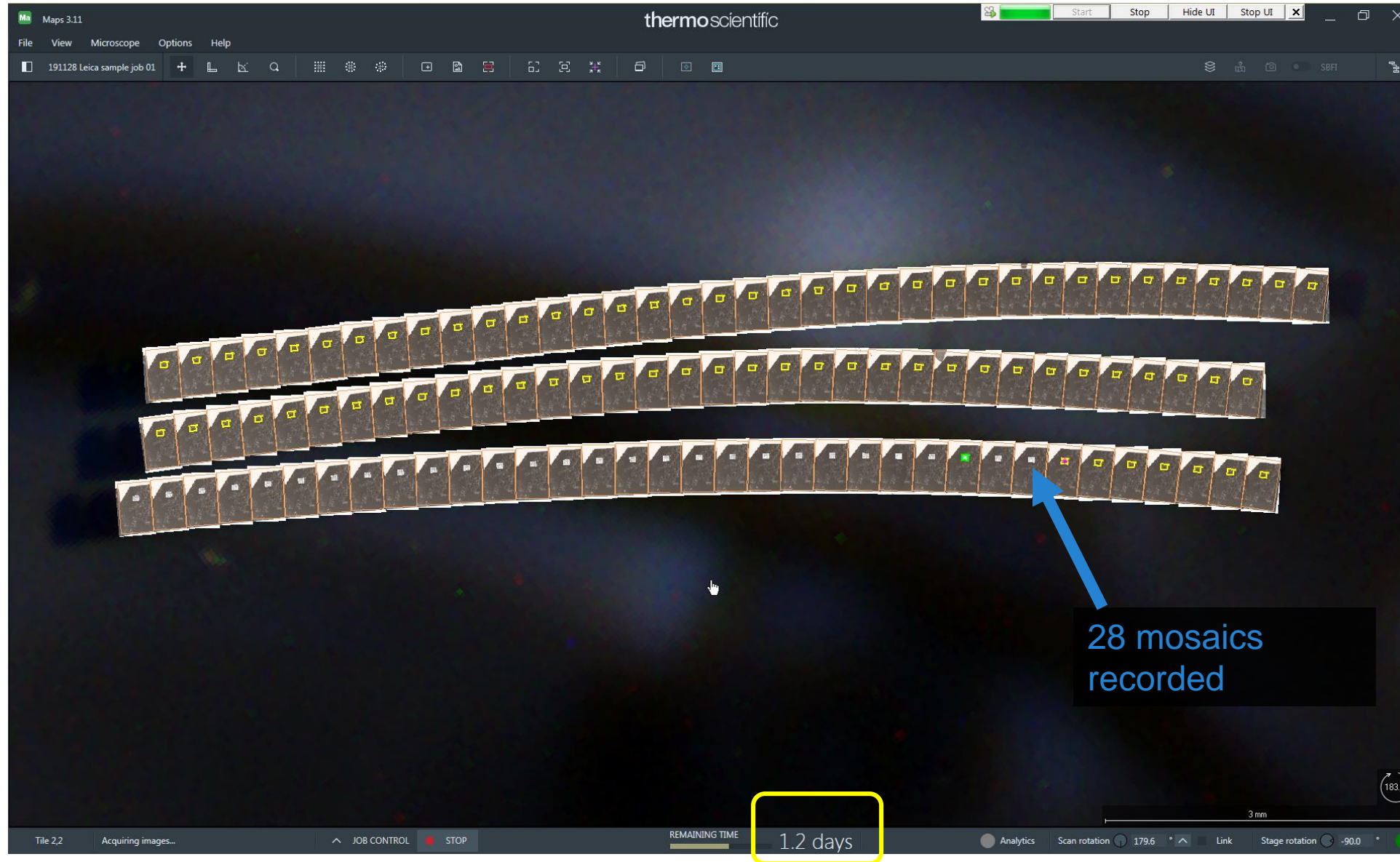
This is the last step in the workflow. It gives control over the acquisition sequence.

- Set the acquisition sequence to “By Section”.
- Make sure the auto functions tile set is acquired first on each section.

Images are then acquired in this sequence:

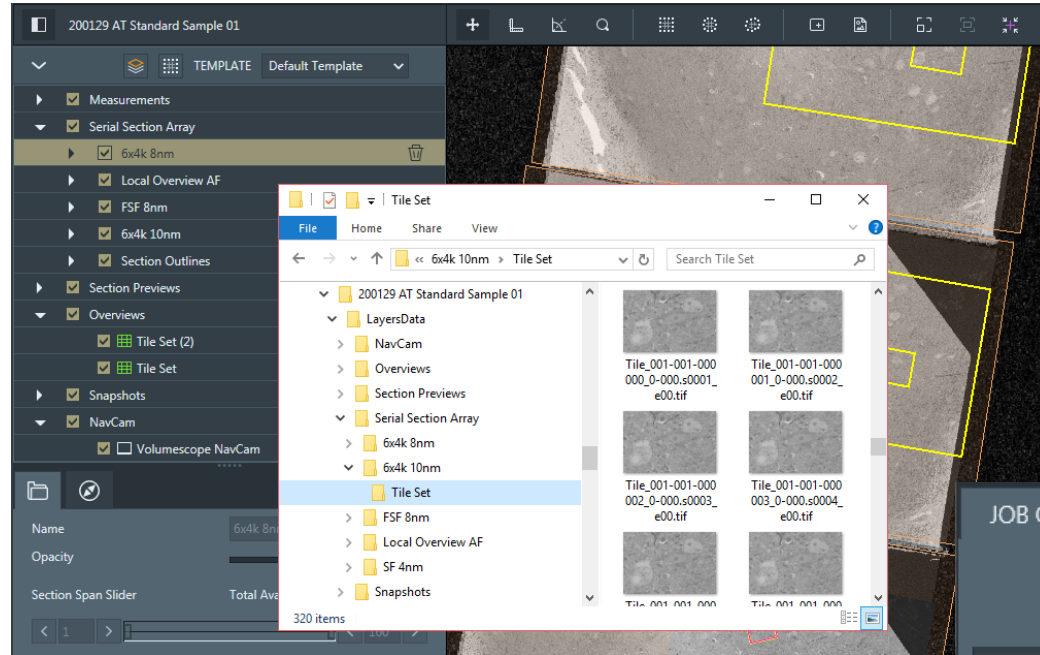
- Section 1: Auto focus, then Mosaic
- Section 2: Auto focus, then Mosaic
- ...
- Section 105: Auto focus, then Mosaic

During acquisition

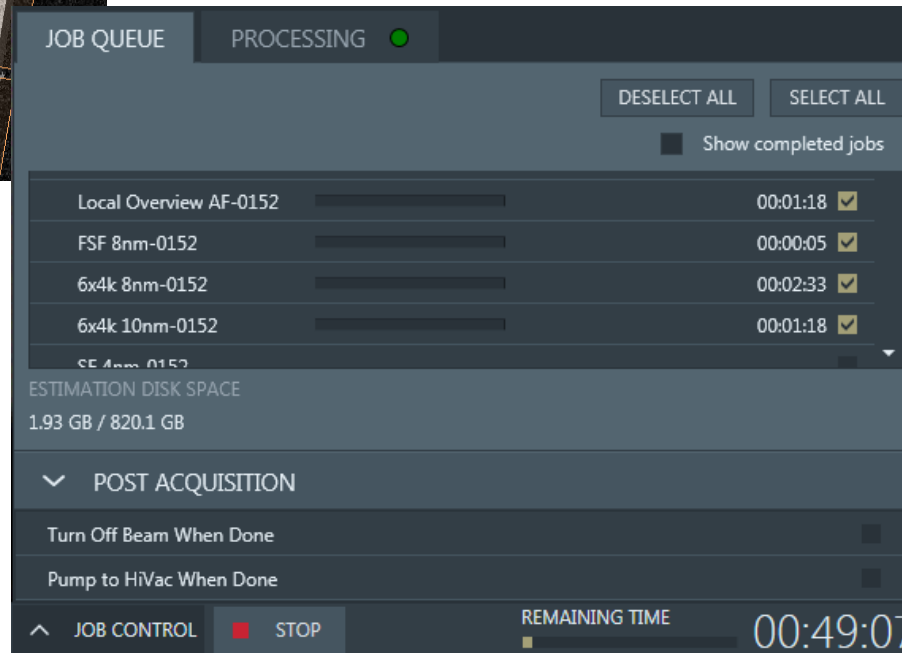


- It is possible to add more Array Tile Sets at any time! Just pause the acquisition and continue from Step 10.
- Likewise, image positions can be changed by click-drag. This can be useful for tracking of features through the 3D volume.
- In case of change in focus, brightness etc during the acquisition, the workflow can be paused and re-initiated after the application of changes.
- Failed or mispositioned images can be reset during or after acquisition. Doing so automatically queues them for re-acquisition.

Data saving and the Job Queue



- The Job Queue shows remaining time in the status bar and the time per tile set when expanded. It also allows reviewing or setting post-acquisition functions like „switch off beam when done“.
- Data are saved into folders on disk in just the same way as arranged in the Layer tree.
- Images are saved in .tif format.
- Mosaics acquired in multiple sections can be stitched into fused .tif images in batch mode.



Troubleshooting and general advice

- Ribbons are not visible in the NavCam image / no Navcam installed.
 - SOLUTION: Find corners of sample holder by navigating in live SEM view and acquire snapshots. Then, use snapshots for orientation while setting up low-resolution SEM overview mosaics of 2x2mm tiles. Even very large areas can be recorded in acceptable time, for instance 5x5cm can be covered within 20 minutes! (28x31 tiles of 1024x864 pixels, 10% overlap, 1 μ s dwell time, 0.5s per tile for stage move).
 - In even larger samples, record several long 1 x N mosaics crisscrossing the stage motion area until sufficient fractions of ribbons or sections are visible. Then, set up one or several SEM overview mosaics that show all sections.
 - In many cases, such low-resolution SEM overview are sufficient for running the Section Finder!
- Section Finder finds less than 90% of sections or more than 10% of false-positives.
 - In case false-sections are detected on tile borders: Use an in-lens detector for acquiring SEM overviews.
The Section Finder falsely recognizes sections on tile borders in SEM overview mosaic(s) where the images have gradients. ETD is known to produce such gradients, while in-lens detectors often produce very flat, gradient-free images.
- If too few sections are recognized, or if the result is overall imprecise, make sure the section-to-background contrast in the image mosaic is higher than the contrast between any other structures in the overview. This can be achieved by choosing suitable accelerating voltage: 2kV is perfect for sections of 50-70nm thickness; reduce the high tension if sections are thinner or weakly stained. Increase to >2kV if sections are thicker. Exclude areas in which false sections are detected from the SEM overview by acquiring several local SEM mosaics instead of one big one.
- I deleted an image (or other object) in Maps. How can I get it back?
 - Not at all. Be careful when selecting items in the layer tree or in the viewer for deleting them! Maps does not have undo, and it doesn't have a recycle bin either.
- I want to run the Section Finder once more in an existing project. What should I be aware of?
 - This can be desirable for example when the array acquisition was set up on only a part of all ribbons of a sample. Be very careful, though: when running the Section Finder a second time in an existing project, all previously found sections are deleted including all images recorded in them! The SOLUTION is to export the SEM overview mosaics into a new Maps project by right-clicking them (or the layer they reside in) in the layer tree and selecting "Export" in the context menu.